HHS Public Access

Author manuscript

Abdom Radiol (NY). Author manuscript; available in PMC 2022 October 07.

Published in final edited form as:

Abdom Radiol (NY). 2022 January ; 47(1): 94–114. doi:10.1007/s00261-021-03324-0.

Magnetic resonance elastography of the liver: everything you need to know to get started

Kay M. Pepin[1,2], **Christopher L. Welle**[1], **Flavius F. Guglielmo**[3], **Jonathan R. Dillman**[4], **Sudhakar K. Venkatesh**[1]

[1]Department of Radiology, Mayo Clinic, 200 First Street SW, Rochester, MN, USA

[2]Resoundant Inc, Rochester, MN, USA

[3]Department of Radiology, Thomas Jefferson University, Philadelphia, PA, USA

[4]Department of Radiology, Cincinnati Children's Hospital Medical Center, University of Cincinnati College of Medicine, Cincinnati, OH, USA

Abstract

Magnetic resonance elastography (MRE) of the liver has emerged as the non-invasive standard for the evaluation of liver fibrosis in chronic liver diseases (CLDs). The utility of MRE in the evaluation of different CLD in both adults and children has been demonstrated in several studies, and MRE has been recommended by several clinical societies. Consequently, the clinical indications for evaluation of CLD with MRE have increased, and MRE is currently used as an add-on test during routine liver MRI studies or as a standalone test. To meet the increasing clinical demand, MRE is being installed in many academic and private practice imaging centers. There is a need for a comprehensive practical guide to help these practices to deliver high-quality liver MRE studies as well as troubleshoot the common issues with MRE to ensure smooth running of the service. This comprehensive clinical practice review summarizes the indications and provides an overview on why to use MRE, technical requirements, system set-up, patient preparation, acquiring the data, and interpretation.

Graphical Abstract

Sudhakar K. Venkatesh, venkatesh.sudhakar@mayo.edu.

Conflict of interest Financial interests Author KP is an employee of Resoundant, Inc. The other authors declare they have no financial interests.

Non-financial interests: None.

Ethical approval This review article did not involve any research involving human participants and/or animals. No ethical approval was needed.

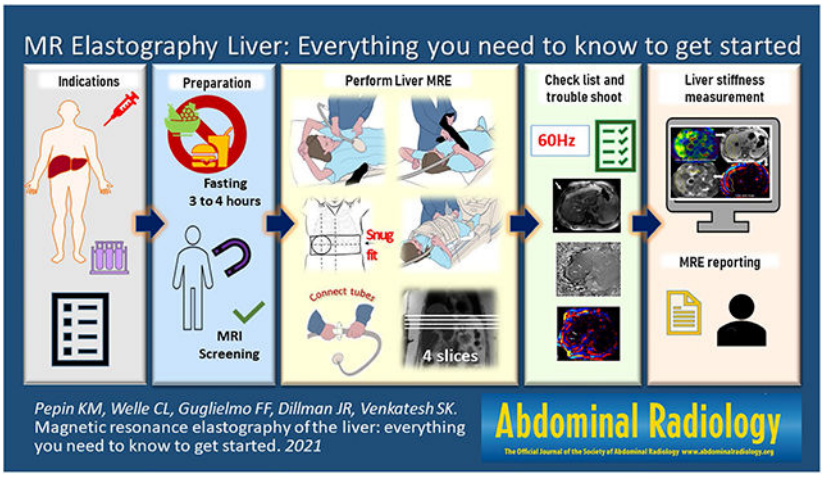

Keywords

Magnetic resonance elastography; Set-up; Preparation; Acquisition; Interpretation

Introduction

Chronic liver disease (CLD) is a growing burden on the global health system and is a major cause of morbidity and mortality [1]. In the USA alone, the projected economic impact on the healthcare system is $1 trillion for 2024 [2]. Histological fibrosis and inflammation evaluations from liver biopsy samples are the currently accepted gold standard for diagnosis and also provide useful information such as the underlying etiology of CLD [3]. While liver biopsy is the standard for diagnosis, there are many technical and practical limitations for widespread use in the growing population with CLD. Widely recognized limitations of liver biopsy include pain, bleeding, sampling error due to small sample size, inter- and intra-reader (pathologist) variability, high cost, liver disease heterogeneity, patient reluctance, and a very small risk of death [4]. Biopsy also can be technically challenging in obese individuals [5]. Due to these factors, repeated biopsies for long-term monitoring and for use in clinical trials for response assessment are typically not practical and noninvasive tests are needed. While fibrosis can be directly visualized at histology, noninvasive techniques can use surrogate biomarkers to indirectly assess fibrosis. One such noninvasive technique is magnetic resonance elastography (MRE). Liver fibrosis is associated with increased extracellular matrix, particularly collagen deposition, leading to increasing rigidity or stiffening of hepatic tissue. MRE utilizes a quantitative phase-contrast-based MRI technique to measure tissue stiffness, thereby indirectly assessing for hepatic fibrosis.

MRE is easily incorporated into standard clinical liver MRI. Studies have demonstrated the utility of MRE in a variety of CLD and MRE is currently regarded as the most accurate non-invasive imaging technique for evaluation of liver fibrosis [6, 7]. In view of the emergence of liver MRE as the non-invasive standard for evaluation of liver fibrosis, a reference guide for setting up and running clinical liver MRE would be useful particularly for institutions considering incorporating MRE into their practice. This review will provide details on what

a radiology practice needs to know to get started with liver MRE, including an overview on why to use MRE, technical requirements, system set-up, patient preparation, acquiring the data, exam interpretation and reporting.

Why use liver MRE?

Liver stiffness quantified by MRE has high diagnostic accuracy for detecting and staging liver fibrosis and is one of the most accurate noninvasive tests currently available [8-10]. Liver MRE is easy to perform and can be easily repeated over time. Technical repeatability of MRE has been rigorously evaluated in multiple studies for within-subject variability in test–retest studies [11-14]. The Quantitative Imaging Biomarker Alliance (QIBA) from the Radiologic Society of North America evaluated the test–retest repeatability of MRE in a meta-analysis and developed a consensus profile on a standardized method for performing MRE to meet a claimed performance: “A measured change in hepatic stiffness of 19% or larger indicates that a true change in stiffness has occurred with 95% confidence” [15, 16]. Given both the excellent accuracy and precision of liver MRE to assess liver stiffness for fibrosis staging, it is recommended by multiple clinical societies, including the American College of Radiology (ACR), the American Association for the Study of Liver Diseases (AASLD), the American Gastroenterological Association (AGA), and the American Academy of Dermatology (AAD) [17-20]. Beginning in 2019, reimbursement for liver MRE is available under the Medicare Category I Current Procedural Terminology® (CPT) code (76391) in the USA. When performed in combination with quantitative imaging to assess liver fat (steatosis) and iron, liver MRI and MRE provides a comprehensive assessment of liver health for the assessment of liver fibrosis, steatosis, and iron.

Indications for liver MRE

The most common clinical indication for liver MRE is evaluation of liver fibrosis. The indications are summarized in Table 1. Liver MRE can be used for detecting, staging, and follow-up evaluation of liver fibrosis for CLD. MRE may be useful in the assessment of treatment response following bariatric surgery [21], weight loss [22], and treatment of chronic viral hepatitis [23]. Additionally, MRE can also be used for longitudinal monitoring in patients receiving drug treatments that may cause liver fibrosis, such as methotrexate for psoriasis treatment [8]. Other emerging indications are differentiation of simple steatosis or non-alcoholic fatty liver (NAFL) from non-alcoholic steatohepatitis (NASH) [21, 24, 25] and in differentiating noncirrhotic portal hypertension (NCPH) from cirrhotic portal hypertension (CPH). NCPH is usually not associated with increased liver stiffness until in the later stages, and this feature is useful in differentiation from CPH [26-28]. Studies have shown that liver stiffness measurement (LSM) with MRE is useful in prediction of decompensation in CLD, individual liver-related clinical events, and risk stratification for CLD-related outcomes [29-34]. LSM with MRE can be useful in predicting decompensation following hepatectomy or radiation treatment [35, 36]. LSM is also useful in identifying patients with clinically significant portal hypertension, including patients with autoimmune liver disease and Fontan patients, or high-risk varices [37-39]. A few studies have shown that increased LSM is associated with increased risk of developing HCC or recurrence following resection [40]. Stiffness of tumors with MRE may be useful as an additional

characteristic for differentiation of benign and malignant tumors of the liver [41]. Other possible applications include evaluation of increased stiffness of the liver from infiltrative diseases such as amyloidosis [42].

What do you need to start clinical MRE?

MRE is available as a hardware and software add-on to existing or new MRI scanners from General Electric (GE Healthcare, Waukesha, WI), Philips (Best, Netherlands), and Siemens (Erlangen, Germany) at both 1.5 T and 3.0 T. LSM is a mechanical property that is not dependent on field strength of the magnet. The LSM measured on 1.5 T or 3.0 T magnets should be similar when all acquisition parameters (patient fasting status, breath holding, shear wave frequency, MRE sequence, and inversion algorithm) are the same. Multiple studies have demonstrated cross-platform and field strength compatibility of MRE [14, 15, 43]. Historically, the technical failure rate was slightly higher at 3.0 T due to the 2D gradient recalled echo-MRE (2D GRE-MRE) sequence being susceptible to T2* effects resulting in poor signal-to-noise ratio (SNR) in tissue with short T2* relaxation times. The use of spin echo-echo planar imaging (SE-EPI)-based MRE acquisition significantly improves the technical success at 3.0 T. The results from both GRE-MRE and SE-EPI MRE are comparable. When selecting a scanner for the MRE application, liver imaging at 1.5 T has an advantage due to fewer artifacts; however, both 1.5 T and 3.0 T will yield accurate, precise, and reproducible results [44, 45].

The MRE application is installed and set-up by the field services engineers from the respective scanner manufacturers. The active driver should be located outside the scan room, preferably in the equipment room (Fig. 1). Placing the active driver near the scanner console is not recommended as the active driver can be quite loud when running. The plastic tube (polyvinyl chloride, 30 ft.) connecting the active driver and passive driver enters the room through the waveguide (a hole in the wall between the equipment room and the scanner). The connecting tube can be coiled and placed in a cabinet or on a shelf when not in use. The passive driver is a rigid, drum-like device that is connected to the active driver via the plastic tube and secured to the body using an elastic strap. Initial training for performing the liver MRE is usually provided by the MRI manufacturer application specialist. Although there are no standard training requirements to perform MRE, adequate training of the MR technicians is essential for performing a high-quality liver MRE. Similarly, radiologists reporting the MRE results would benefit from training from experts for avoiding interpretation errors.

How to use the MRE phantom

An MRE phantom (Resoundant, Inc., Rochester, MN) is included in the accessories kit and can be used for training, allowing users to verify that the MRE system is functioning correctly and to perform any necessary troubleshooting. When an MRE phantom is available, a phantom scan can be performed periodically or as part of new MRE user training; however, there are no current guidelines on how often a phantom scan should be performed. Phantom scanning procedures can be found under QIBA guidelines [16]. The phantom MRE scan parameters are different from human MRE scans; however, the driver frequency is still 60 Hz. The two important differences are driver amplitude is set

at or below 10% and plane of acquisition is in the coronal imaging plane (patient scans are performed in the axial plane). Sample phantom results for normal and failed exams are included in Fig. 2. When evaluating the phantom results, users should consider all standard outputs (magnitude images, wave images, and elastograms). Normal phantom results include subtle or barely visible shear waves through the phantom on magnitude images, red/blue waves appearing in concentric circles in the color wave image, and a homogenous shear stiffness of approximately 3 kPa (acceptable range 2–4 kPa, based on manufacturer recommendations). The phantom stiffness is not calibrated, but once a baseline stiffness is established, future scans should remain within ± 10%. The stiffness measured with the phantom is expected to remain stable for many years provided the phantom is not deformed or the seal is not broken.

There are three common types of poor phantom results including high amplitude, low amplitude, and no amplitude. In the case of high amplitude, the wave image appears oversaturated (the shear waves appear more yellow and turquoise blue instead of deep red and blue colors, Fig. 2 second column from the left) and the magnitude image may even include the appearance of waves. This is likely due to a failure to reduce the amplitude of the active driver to 10% for the phantom scan. Low amplitude appears as undersaturated or dark waves and lack of a high confidence region or inhomogeneous stiffness in the elastogram (Fig. 2, third column from the left). This could be due to improper phantom setup (the belt around the passive driver and the phantom used for securing is not tight enough) or a problem with the MRE active driver. In the case of no amplitude (Fig. 2, right column), there are no visible shear waves in the wave image and a completely masked out elastogram due to low confidence. In this case, it is important to ensure that the active driver is on, the tube is connected between the active and passive drivers, and all the sequence parameters are optimized.

Patient preparation

Proper patient preparation is essential to achieve a successful and accurate exam. Patients must be fasting for a minimum of 3 to 4 h before the MRE exam. A significant increase in postprandial liver stiffness (21% ± 15%) can be observed in patients with CLD and underlying fibrosis within 30 min of a meal [46]. This change in stiffness was not observed in healthy volunteers. Failure to follow the fasting recommendations may result in over-staging of liver fibrosis (Fig. 3). Similar fasting status should be observed in the follow-up MRE exams so that the changes in stiffness values are correctly interpreted.

Positioning of passive driver

The rigid passive driver should be positioned over the right hepatic lobe, with the superior–inferior position centered at the level of the xiphoid process of the sternum, and the left–right position centered over the right midclavicular line (Fig. 4). The positioning of the large flexible driver yields good results when the edge of the driver rests on the table on the patient’s right side, wrapping along the anterior of the body toward the patient’s midline. Superior/inferior positioning remains centered at the level of the xiphoid process. The goal is to position the passive driver over the largest portion of the liver, and the positioning may

need to be adjusted for some patients depending on individual anatomy. MR technicians must ensure that the belt securing the passive driver in place is as tight as possible while still allowing the subject to breathe comfortably. The belt should be tightened while the subject is in end-expiration. This is especially important for obese subjects. For very small patients and pediatric patients, towels or other cloth can be used to eliminate air gaps between the passive driver and body surface. Once the passive driver is positioned and connected to the active driver, the localizer and calibration scans for liver MRE should be obtained. If MRE is performed at the end of a liver MRI study, a repeat localizer scan should be obtained to locate the position of the driver for determining the positioning of slices.

Performing the MRE sequence: acquiring the data

Liver MRE data can be acquired during a full abdominal MRI, or as part of a limited liver MRI protocol which may include MR sequences for liver iron and fat quantification. Liver MRE can be performed before or after gadolinium-based contrast material administration as studies have shown that gadolinium-based contrast materials do not affect LSM by MRE [47, 48]. The advantage of performing the scan before contrast is optimization of workflow to allow for the post-processing of imaging to occur while obtaining any post-contrast imaging. If the MRE exam fails, the acquisition can be repeated. However, if the liver MRE is obtained post-contrast, the increased signal intensity can produce higher-quality elastograms in which a larger area of the liver is uncovered by the confidence map resulting in more liver parenchyma available to make LSMs [49].

Breath holds must be performed at end-expiration. Multiple studies have found higher reproducibility when performed at end-expiration due to a more reproducible liver position, and a recent study found elevated liver stiffness values when performed at inspiration particularly in patients with liver fibrosis [50, 51]. The scout or localizer image used for slice selection must also be performed at end-expiration. Additionally, the localizer image can typically be used to determine the location of the passive driver, visible as an indentation or flattening of the subcutaneous tissue. The driver should be repositioned before the scan if not located over the liver. Position the sections in the widest cross-section of the liver, approximately 2–10 cm away from the superior and inferior margins of the liver (Fig. 5). Typically, four sections are obtained. Additionally, signal in the liver can be improved by avoiding sections too close to the lung, particularly for GRE sequences.

Typical MRE pulse sequences parameters are provided in Table 2. The recommended parameters can also be found in the QIBA profile, which is updated on a regular basis [16]. There are a few parameters that may be adjusted to improve image quality and several parameters that should not be changed (Table 3). Many of the pulse sequence parameters should not be adjusted, including the vibration frequency (standardized at 60 Hz), the motion-encoding gradient (MEG) and MEG direction, the number of phase offsets, and the fractional encoding. Liver tissue is a viscoelastic material and the stiffness calculated from the propagation of shear waves is dependent on the frequency of the applied motion. For clinical liver MRE, stiffness thresholds have been established at 60 Hz, and the frequency should not be changed, as an increase (decrease) in frequency increases (decreases) measured shear wave speed. Similarly, the field of view should be kept consistent between

repeat scans or for the course of a clinical trial. Some parameters that can be adjusted to improve image quality include the driver amplitude and the echo time (TE). The TE should be set to an in-phase value to improve signal, which may vary by pulse sequence and field strength [16].

The driver amplitude determines the intensity of shear waves applied to the liver and can be increased or decreased depending on the patients' body habitus and the passive driver used (rigid or flexible) (Table 4). These amplitude recommendations are based on our experience in over 15,000 MRE exams. If the amplitude setting is too low, shear wave penetration in the liver will be low and will result in a low-quality exam (Fig. 6). Alternatively, if the amplitude setting is too high, the patient may experience some discomfort and the excessive motion in the liver and result in signal loss near the driver and a poor-quality exam. This is particularly important in small children. Recommendations for amplitudes for pediatric patients are provided in Table 5. These pediatric amplitude recommendations are based on our experience in performing > 1500 pediatric MRE exams. A recent study compared different driver amplitudes on LSM in pediatrics and emphasized the importance of optimizing amplitude according to pediatric size. While LSM showed good reliability between different amplitudes, regions of interest (ROI) size can be reduced if the amplitude is too high or too low [52]. Further studies are needed using optimized amplitudes.

After completion of the exam, the performing MRI technologist (or alternatively the supervising MRI radiologist) should immediately review the images to ensure diagnostic quality and the MRE should be repeated if necessary. All the raw and post-processed images should be reviewed. Technologists should check the magnitude images for artifacts (ex: excessive respiratory motion) and the presence of a signal void in the subcutaneous tissue directly below the passive driver, the raw phase images for the presence of shear waves, the reconstructed wave images for adequate shear wave propagation, and the elastogram to confirm an adequate region of high confidence. The phase images are the raw phase difference from the positive and negative motion encodings, displaying the tissue wave displacement [53]. The reconstructed wave images are typically displayed in color and have been processed to remove phase wrapping (phase discontinuities). A critical step is to make sure that the shear waves are delivered and are propagating through the liver. This can be verified by observing signal loss in the subcutaneous fat just below the passive drive, propagating shear waves through the liver on phase images, and planar wave propagation on wave images (Fig. 7). Planar wave propagation can be seen as parallel lines of shear wave motion (orange/blue lines in color image or light gray/dark gray in phase or grayscale wave image) and represents propagation of the waves in the imaging plane. Out-of-plane wave propagation, seen as broken lines, can lead to over- or under-estimation of shear stiffness.

Troubleshooting tips for MR technologists

The reported technical success rate of MRE is very high (95–100%), including in children [54-56]. However, there are a few causes of technical failure or reduced image quality, including hepatic iron overload, bowel interposition, improper slice selection, respiratory motion, operator error, or hardware failure.

High iron content in the liver causes loss of MR signal from the liver parenchyma, which may result in poor SNR and a poor quality or uninterpretable MRE result. It should be noted that shear waves still propagate through the liver with iron overload but are not visualized with MRE sequence when liver parenchymal signal is low. A GRE MRE pulse sequence technique is widely used with good diagnostic performance; however, it is sensitive to short T_2* relaxation times caused by iron overload or other susceptibility effects, particularly at higher magnetic field strengths (i.e., 3.0 T vs. 1.5 T). The signal loss is greater at longer TE and less at shorter TE. An MRE sequence with shorter TE would benefit from improved signal in subjects with iron overload. Accordingly, MRI manufacturers have implemented a SE-EPI MRE technique which is much less affected by T_2* relaxation effects, has a shorter TE, and therefore should ideally be used in all 3.0 T MRI systems where T2* relaxation effects are more prevalent. SE-EPI is also available on some systems at 1.5 T and can be used. In a meta-analysis, overall MRE with both GRE and SE-EPI sequences had excellent technical success rates, but the SE-EPI MRE technique had a higher technical success rate than with the conventional GRE sequence (98.0% vs. 94.2%) [45]. Iron overload in the liver can sometimes be recognized in the scout image. In normal liver, the signal intensity between the liver, spleen, and kidney is similar, whereas in the case of hepatic iron overload, the liver will appear darker. There are no established thresholds of R_2* that are predictive of exam failure for either GRE or SE-EPI acquisitions [57-59].

If shear waves are present but the amplitude is low, denoted by visible waves in the phase/wave images but a small or absent region of high confidence in the elastogram, the exam should be repeated to obtain MRE with shear waves of adequate amplitude. Ensure a firm connection between the passive and active driver tubes. The belt securing the passive driver to the abdomen should be tightened at end-expiration. Additionally, if the subject is obese and/or has a large waist circumference, the amplitude can be increased as outlined in Table 4. If no shear waves were visible, confirm the tube is connected, the active driver is on, and the amplitude settings are correct. The technician can stand next to the active driver during the scan to feel/listen for vibrations. If no vibrations are felt, contact the MR service representative. A checklist for MR technicians is included in Fig. 8.

Uncommonly, the interposition of gas-filled bowel between the passive driver and the liver may result in a failed exam due to low-amplitude shear waves. The passive driver may be repositioned, and the exam repeated. Additionally, if a poor-quality exam is obtained due to improper slice selection or respiratory motion, the exam should be repeated with proper slice selection and the patient should be encouraged to hold their breath consistently. In patients with altered anatomy such as situs inversus, post-hepatic resection or living liver donor (segmental) transplants, the driver should be positioned as close to the remnant liver as possible which could be either left side, midline, or further right lateral. A troubleshooting algorithm is illustrated in Fig. 9.

Post-processing

Following the acquisition, the magnitude and phase images are produced on the scanner and represent the raw data. The magnitude images provide anatomic information, and the phase images can be used to visually assess the presence of shear waves in the liver. These

images can be immediately assessed by the technician to confirm the technical success of the acquisition. Shear waves should be present in the phase image, and the magnitude image should be reviewed to confirm the presence of abdominal wall signal void, for proper slice selection, and for artifacts such as respiratory motion.

Post-processed images are created from the raw images using a multimodel direct inversion algorithm (MMDI), which is relatively consistent across scanner manufacturers [60]. Several additional image series are created and available post-processed series varies by scanner manufacturer (Table 6; Fig. 10). Table 6 describes the data that each scanner can export for MRE results. In some cases, users may need to manually select to have these images included in the output. The most consistent output images are a grayscale elastogram (0–8 kPa) and a grayscale elastogram with confidence map overlay. The grayscale elastograms provide quantitative stiffness values and should be used for analysis. The confidence map is a tool to assist in locating regions of reliable information for ROI placement. Additional post-processed images include grayscale and color wave images, a grayscale confidence map, and color elastograms with and without the confidence map overlay. Color elastograms are non-quantitative and should not be used to measure stiffness. They are useful for identifying hot spots, which should be avoided when making measurements. They also provide a qualitative overview of the liver for a rapid visual assessment of whether the measured liver stiffness will be normal or elevated. These post-processed images may require a manual step to generate on the scanner. Also, in some cases, a color elastogram on an expanded stiffness scale from 0 to 20 kPa is created. This image may be useful in appreciating heterogeneity in very stiff livers but is typically not needed for routine clinical purposes.

Liver stiffness measurement (LSM)

After assuring a good-quality exam, ROI can be drawn to measure liver stiffness. To reduce sampling error, the largest possible volume of liver parenchyma should be included within the ROI. Either manual or automated ROI measurements can be obtained, as further detailed later in this paper. General guidelines for ROI drawing include avoiding the liver edge (approximately 1 cm), the gallbladder fossa, and large vessels. Additionally, only areas with good waveforms should be included in measurements. When making manual LSMs, this can be performed at the MR scanner or directly on PACS or a separate workstation for optimal workflow. The process for manual measurement varies slightly depending on the availability of images and features of the PACS/workstation such as availability of a copy/paste function. We describe three common methods for making manual measurements below.

For systems providing a confidence map and copy and paste function, the first step in making measurements is to draw an ROI on the elastogram with confidence map, while keeping the ROI within the valid or non-hashed out region (Fig. 11). Next, this ROI is copied to the magnitude image, where modifications can be made to ensure the ROI is within the liver and avoiding major vessels, liver edge, and fissures. The ROI is then copied to the color wave image to ensure only good-quality waves are being sampled. Finally, the ROI is transferred to the grayscale elastogram to obtain the liver stiffness. With some

vendors, the color stiffness map may be scaled so that LSM measurement can be performed similar to that on a grayscale stiffness map.

If no confidence map is obtained but a copy and paste function is available (Fig. 12), the first step is drawing an ROI on the magnitude image. This ROI should then be copied to the color wave image, with modifications made to assure only sampling of good-quality waves. The final step is to copy to the grayscale or color elastogram to obtain the stiffness measurement. On elastogram images, artifactual areas of elevated liver stiffness called “hot spots” are generally avoided.

For systems that provide a confidence map but no copy and paste function, the first step in making measurements is to correlate the grayscale elastogram with confidence map image with the magnitude image (Fig. 13). Ensure that appropriate areas in the liver are excluded such as the peripheral liver and large blood vessels. Some systems provide a “localizer” function for this purpose. Next, the wave image should be reviewed to include only good-quality waves. Then, the color elastogram is reviewed to avoid “hot spots” created by wave distortion or the adjacent passive driver. After reviewing all four series, freehand ROI measurements are made on the grayscale elastogram image.

This process is repeated for all four slices obtained. The weighted arithmetic mean is then calculated, which considers the liver stiffness of each slice and the area sampled. The formula is as follows: Weighted arithmetic mean = $(m_1 w_1 + m_2 w_2 + m_3 w_3 + m_4 w_4) \div (w_1 + w_2 + w_3 + w_4)$, where “m” equals the mean liver stiffness for that particular slice and “w” equals the ROI size in pixels in mm^2 or cm^2. The weighted arithmetic mean can then be used to correlate with fibrosis stage (Table 7) [61].

MRE has excellent reproducibility and inter-operator consistency for drawing ROIs and reporting stiffness measurements, with intra-class correlation coefficients (ICC) of 97–100% [62]. A recent comparison between manual and automated processing for LSM in pediatric patients reported ICC = 0.99 for inter-reader agreement and ICC = 0.988 for agreement between manual and automated processing [63]. One study concluded that operators should be trained to acquire ROIs consistently in repeat examinations [40] and automated analysis may be beneficial for this process [64, 65].

Confounders of liver stiffness measurement

LSM with MRE is a surrogate marker for liver fibrosis in CLD. In the clinical context of CLD and abnormal liver function tests, increased LSM is suggestive of liver fibrosis. In most CLD, particularly in the earlier course of the disease, active and chronic inflammation as well as fibrosis often coexist. Inflammation can also cause increased liver stiffness and therefore can affect the accuracy of fibrosis staging, especially in early stages of CLD. As untreated inflammation leads to fibrosis, it is best regarded as a continuum with significant overlap during the course of the disease.

The differences in liver stiffness between adjacent fibrosis stages, particularly early stages (F1–2), are small, and the presence of chronic inflammation can further decrease the accuracy for differentiation of the adjacent stages of fibrosis. This limitation on accuracy of

differentiating early stages of fibrosis is a universal phenomenon with non-invasive imaging-based techniques, including transient elastography and ultrasound shear wave elastography. The performance of liver MRE is still very good in early stages of fibrosis, with accuracy > 0.85 reported in most published series. With MRE technical advances in the future, it may be possible to differentiate more reliably inflammation from fibrosis and between adjacent fibrosis stages in early disease.

However, acute inflammation such as acute hepatitis or acute flare in CLD is a confounder and performing liver MRE for fibrosis staging in the setting of acute inflammation should be avoided if possible. Similarly, acute biliary obstruction and venous congestion secondary to congestive cardiac failure can increase liver stiffness and these coexisting confounders should be ruled out or MRE should be specifically avoided for fibrosis staging in these situations. In the case of congestive hepatopathy (post-Fontan surgery, tricuspid regurgitation, congestive cardiac failure, etc.), serial monitoring may help in detection of increasing stiffness which indicates worsening congestion or progression of fibrosis. Uncommonly, diffuse infiltrative disorders that cause increased liver stiffness may mimic CLD. Examples include amyloidosis, Gaucher disease, and diffuse metastases. Careful evaluation of the clinical presentation and other imaging studies would usually help rule out these conditions. Liver MRE for fibrosis evaluation should also be avoided when another diffuse infiltrative disorder is known to exist such as amyloidosis which also causes increased liver stiffness. Liver biopsy may need to be performed for diagnosis of CLD when the exact etiology of the CLD is not known.

While there are many pathologic conditions that can increase liver stiffness, a normal liver stiffness is most reassuring evidence that there is no significant liver fibrosis as there are no known pathologic conditions that significantly decrease liver stiffness. Fatty change in the liver does not systematically affect LSM with MRE [24, 66-68]. In a longitudinal study evaluating the effectiveness of a therapeutic agent that reduces liver fat showed that there was no significant change in liver stiffness even when liver fat content reduced significantly by more than 30% in treated subjects suggesting that steatosis had no significant impact on liver stiffness measured with MRE. However, one study noted that liver stiffness in pediatric patients was associated with multiple patient-specific factors including fat fraction [69]. The study showed a small decrease in stiffness with increasing fat content. The relationship between hepatic steatosis and liver stiffness in pediatric subjects needs to be further clarified in future large cohort studies. Occasionally significantly elevated liver stiffness may be seen with MRE in a morphologically normal liver on ultrasound, CT, and routine MRI sequences particularly in patients with NAFLD. Advanced liver fibrosis may be present in asymptomatic patients with a morphologically normal liver and without any abnormal liver function tests. In such scenarios, acute inflammation should be ruled out by correlating with liver function tests.

During longitudinal monitoring of a CLD, significant changes in liver stiffness can occur in patients showing response to treatment over weeks to months. The significant change in the stiffness can be due to improvement in both inflammation and fibrosis when present initially. The improvement in inflammation occurs within a short period of time typically over weeks compared to fibrosis which takes longer time to improve and typically occurs

over months. As active or chronic inflammation and fibrosis represent a continuum of disease, any improvement in stiffness should be regarded as a response to treatment. QIBA guidelines recommend a LSM change of > 19% as significant change and this can be applied for reporting significant change in stiffness.

Potential limitations of liver MRE

There are no specific contraindications to MRE beyond the standard contraindications to MRI; however, there are a few factors that may affect the reliability or technical success of MRE-based LSM. High liver iron content is the most common cause of technical failure for MRE exams, addressed in many studies and meta-analyses [45, 70, 71]. The presence of ascites has been found to not hinder the generation and imaging of shear waves in the liver and the technical success of MRE [67, 72, 73]. Occasionally, a large amount of ascites can cause difficulty in radiofrequency penetration, leading to poor image quality in all types of abdominal MRI, including MRE (i.e., dielectric effect) [74]. Multiple studies have demonstrated the high technical success rate of MRE in obese subjects with rare failures [21, 56, 75]. The limiting factor in obese individuals is not body mass index (BMI) but specifically the waist circumference and the ability of the patient to fit in the MRI scanner [75]. Metallic stents that are in or near liver may be a potential source of susceptibility artifacts interfering with MRE assessment of liver stiffness. These can be identified on localizer or anatomical MR sequences performed before MRE and potentially avoided.

Technical innovations

Recent technical innovations have occurred in multiple areas related to liver MRE, including applications in the hardware, pulse sequence, inversion algorithm, automated analysis, and parameter specification to better diagnose the presence of liver disease. A rigid passive driver is the current standard for introducing shear waves into the liver; however, this rigid driver can be uncomfortable for some patients and challenging to set up correctly. A new, ergonomic, flexible driver has been developed to better conform to the curvature of the body surface and produce more uniform shear waves in the liver [50].

Advances in the MRE pulse sequence are also an active area of research. Patients with CLD often suffer from comorbidities that may limit their ability to hold their breath during the MRE exam. Respiratory motion may degrade the consistency of the MRE phase-encoded data [76]. Recent studies demonstrated the feasibility of a free-breathing and respiratory-triggered MRE acquisition, which is well suited for patients with breath-holding limitations and pediatric patients [76-78]. The addition of compressed sensitivity encoding (SENSE) allows for an approximately 50% reduction in breath-hold times with minimal bias [79].

Significant research efforts have evaluated the use of 3D MRE (i.e., shear wave tracking in the *x*-, *y*-, and *z*-direction) in multiple clinical applications [50, 80-84]. 3D MRE may be more precise than 2D MRE due to the ability to resolve shear wave propagation in three directions instead of a single plane in 2D, allowing for the improved visualization of shear wave propagation in complex organs. Stiffness values from 3D MRE are typically lower than 2D [81], and future work is needed to establish robust thresholds for diagnosis.

Multiple studies have demonstrated the potential added benefit of mechanical parameters from 3D MRE to help noninvasively diagnose NASH [21, 85]. The combination of parameters including $|G^*|$ and the damping ratio from MRE and MRI-PDFF can predict the NAFLD activity score (NAS).

Automated analysis of liver MRE showed excellent agreement with expert readers and could decrease analysis time and improve read reliability [86-88]. Multiple independent studies have demonstrated the excellent reliability and performance of an automated liver elasticity calculation (ALEC), also referred to as MREplus$^+$ (Resoundant, Inc., Rochester, MN). In a pediatric cohort with autoimmune liver disease, correlation between manual reads and automated analysis was very strong (ICC = 0.988) [63]. In a pediatric population with NAFLD, the correlation between automated analysis and each of two expert reading centers (p = 0.9, 0.79) was comparable to the correlation between manual measurements at the two centers (p = 0.83) [89]. Automated analysis for MRE and MRI-PDFF was used to predict biopsy-diagnosed NASH with an AUROC of 0.87 [90].

Conclusion

MRE has been extensively validated and is a valuable tool for the assessment of liver stiffness. It can be incorporated into most new or existing MR scanners and, once the staff has been trained, is rather simple to perform and troubleshoot. Interpreting and reporting is straightforward, with well-established values correlating with stages of fibrosis. Given the increasing incidence of CLD, every radiology practice should consider if MRE is a tool that it can offer its patients.

Funding

Dr. Dillman acknowledges liver-related research support from Philips Healthcare, GE (General Electric) Healthcare, Perspectum Ltd, Siemens Healthineers and Canon Medical Solutions. Dr. Venkatesh acknowledges support from National Institute of Health Grant (EB001981) and U.S. Department of Defense grant (W81XWH-19–1-0583-01). Drs. Pepin, Welle and Guglielmo did not receive support from any organization for the submitted work

References

1. Collaborators GBDC (2020) The global, regional, and national burden of cirrhosis by cause in 195 countries and territories, 1990–2017: a systematic analysis for the Global Burden of Disease Study 2017. Lancet Gastroenterol Hepatol 5 (3):245–266. doi:10.1016/S2468-1253(19)30349-8 [PubMed: 31981519]
2. Estes C, Razavi H, Loomba R, Younossi Z, Sanyal AJ (2018) Modeling the epidemic of nonalcoholic fatty liver disease demonstrates an exponential increase in burden of disease. Hepatology 67 (1):123–133. doi: 10.1002/hep.29466 [PubMed: 28802062]
3. Berger D, Desai V, Janardhan S (2019) Con: Liver Biopsy Remains the Gold Standard to Evaluate Fibrosis in Patients With Nonalcoholic Fatty Liver Disease. Clin Liver Dis (Hoboken) 13 (4):114–116. doi: 10.1002/cld.740 [PubMed: 31061705]
4. Davison BA, Harrison SA, Cotter G, Alkhouri N, Sanyal A, Edwards C, Colca JR, Iwashita J, Koch GG, Dittrich HC (2020) Suboptimal reliability of liver biopsy evaluation has implications for randomized clinical trials. J Hepatol 73 (6):1322–1332. doi: 10.1016/j.jhep.2020.06.025 [PubMed: 32610115]
5. Barsic N, Lerotic I, Smircic-Duvnjak L, Tomasic V, Duvnjak M (2012) Overview and developments in noninvasive diagnosis of nonalcoholic fatty liver disease. World J Gastroenterol 18 (30):3945–3954. doi: 10.3748/wjg.v18.i30.3945 [PubMed: 22912545]

6. Selvaraj EA, Mozes FE, Jayaswal ANA, Zafarmand MH, Vali Y, Lee JA, Levick CK, Young LAJ, Palaniyappan N, Liu CH, Aithal GP, Romero-Gomez M, Brosnan MJ, Tuthill TA, Anstee QM, Neubauer S, Harrison SA, Bossuyt PM, Pavlides M, Investigators L (2021) Diagnostic accuracy of elastography and magnetic resonance imaging in patients with NAFLD: A systematic review and meta-analysis. J Hepatol 75 (4):770–785. doi: 10.1016/j.jhep.2021.04.044 [PubMed: 33991635]

7. Lefebvre T, Wartelle-Bladou C, Wong P, Sebastiani G, Giard JM, Castel H, Murphy-Lavallee J, Olivie D, Ilinca A, Sylvestre MP, Gilbert G, Gao ZH, Nguyen BN, Cloutier G, Tang A (2019) Prospective comparison of transient, point shear wave, and magnetic resonance elastography for staging liver fibrosis. Eur Radiol 29 (12):6477–6488. doi: 10.1007/s00330-019-06331-4 [PubMed: 31278577]

8. Cui J, Ang B, Haufe W, Hernandez C, Verna EC, Sirlin CB, Loomba R (2015) Comparative diagnostic accuracy of magnetic resonance elastography vs. eight clinical prediction rules for non-invasive diagnosis of advanced fibrosis in biopsy-proven non-alcoholic fatty liver disease: a prospective study. Alimentary Pharmacology and Therapeutics 41:1271–1280 [PubMed: 25873207]

9. Hsu C, Caussy C, Imajo K, Chen J, Singh S, Kaulback K, Le MD, Hooker J, Tu X, Bettencourt R, Yin M, Sirlin CB, Ehman RL, Nakajima A, Loomba R (2019) Magnetic resonance vs. transient elastography analysis of patients with nonalcoholic fatty liver disease: a systematic review and pooled analysis of individual participants. Clinical Gastroenterology and Hepatology 17:630–637 [PubMed: 29908362]

10. Liang Y, Li D (2020) Magnetic resonance elastography in staging liver fibrosis in non-alcoholic fatty liver disease: a pooled analysis of the diagnostic accuracy. BMC Gastroenterol 20 (1):89. doi: 10.1186/s12876-020-01234-x [PubMed: 32252641]

11. Yoon JH, Lee JM, Woo HS, Yu MH, Joo I, Lee ES, Sohn JY, Lee KB, Han JK, Choi BI (2013) Staging of hepatic fibrosis: comparison of magnetic resonance elastography and shear wave elastography in the same individuals. Korean Journal of Radiology 14 (2):202–212 [PubMed: 23483022]

12. Yoon JH, Lee JM, Joo I, Lee ES, Sohn JY, Jang SK, Lee KB, Han JK, Choi BI (2014) Hepatic fibrosis: prospective comparison of MR elastography and US shear-wave elastography for evaluation. Radiology 273 (3):772–782 [PubMed: 25007047]

13. Shire NJ, Yin M, Chen J, Railkar RA, Fox-Bosetti S, Johnson SM, Beals CR, Dardzinski BJ, Sanderson SO, Talwalkar JA, Ehman RL (2011) Test–retest repeatability of MR elastography for noninvasive liver fibrosis assessment in Hepatitis C. Journal of Magnetic Resonance Imaging 34:947–955 [PubMed: 21751289]

14. Trout AT, Serai S, Mahley AD, Wang H, Zhang Y, Zhang B, Dillman JR (2016) Liver stiffness measurements with MR elastography: agreement and repeatability across imaging systems, field strengths, and pulse sequences. Radiology 281 (3):793–804 [PubMed: 27285061]

15. Serai SD, Obuchowski NA, Venkatesh SK, Sirlin CB, Miller FH, Ashton E, Cole PE, Ehman RL (2017) Repeatability of MR elastography of liver: a meta-analysis. Radiology 285 (1):92–100 [PubMed: 28530847]

16. QIBA.

17. Lim JK, Flamm SL, Singh S, Falck-Ytter YT, Association CGCo-tAG (2017) American Gastroenterological Association Institute Guideline on the role of elastography in the evaluation of liver fibrosis. Gastroenterology 152:1536–1543 [PubMed: 28442119]

18. Horowitz JM, Kamel IR, Arif-Tiwari H, Asrani SK, Hindman NM, Kaur H, McNamara MM, Noto RB, Qayyum A, Lalani T (2017) ACR Appropriateness Criteria Chronic Liver Disease. Journal of the American College of Radiology 14:S103–S117 [PubMed: 28473066]

19. Chalasani N, Younossi Z, Lavine JE, Charlton M, Cusi K, Rinella M, Harrison SA, Brunt EM, Sanyal AJ (2018) The diagnosis and management of nonalcoholic fatty liver disease: Practice guidance from the American Association for the Study of Liver Diseases. Hepatology 67 (1):328–357. doi: 10.1002/hep.29367 [PubMed: 28714183]

20. Menter A, Gelfand JM, Connor C, Armstrong AW, Cordoro KM, Davis DMR, Elewski BE, Gordon KB, Gottlieb AB, Kaplan DH, Kavanaugh A, Kiselica M, Kivelevitch D, Korman NJ, Kroshinsky D, Lebwohl M, Leonardi CL, Lichten J, Lim HW, Mehta NN, Paller AS, Parra SL, Pathy AL, Prater EF, Rahimi RS, Rupani RN, Siegel M, Stoff B, Strober BE, Tapper EB, Wong EB, Wu JJ, Hariharan V, Elmets CA (2020) Joint American Academy of Dermatology–National

Psoriasis Foundation guidelines of care for the management of psoriasis with systemic nonbiologic therapies. J Am Acad Dermatol 82 (6):1445–1486. doi: 10.1016/j.jaad.2020.02.044 [PubMed: 32119894]

21. Allen AM, Shah VH, Therneau TM, Venkatesh SK, Mounajjed T, Larson JJ, Mara KC, Kellogg TA, Kendrick ML, McKenzie TJ, Greiner SM, Li J, Glaser KJ, Wells ML, Gunneson TJ, Ehman RL, Yin M (2020) Multiparametric Magnetic Resonance Elastography Improves the Detection of NASH Regression Following Bariatric Surgery. In: Hepatol Commun, vol 4. vol 2. pp 185–192. doi: 10.1002/hep4.1446 [PubMed: 32025604]
22. Patel NS, Hooker J, Gonzalez M, Bhatt A, Nguyen P, Ramirez K, Richards L, Rizo E, Hernandez C, Kisseleva T, Schnabl B, Brenner D, Sirlin CB, Loomba R (2017) Weight loss decreases magnetic resonance elastography estimated liver stiffness in nonalcoholic fatty liver disease. Clinical Gastroenterology and Hepatology 15:463–464 [PubMed: 27712981]
23. Higuchi M, Tamaki N, Kurosaki M, Inada K, Kirino S, Yamashita K, Hayakawa Y, Sekiguchi S, Osawa L, Takaura K, Maeyashiki C, Kaneko S, Yasui Y, Tsuchiya K, Nakanishi H, Itakura J, Enomoto N, Izumi N (2020) Changes of liver stiffness measured by magnetic resonance elastography during direct-acting antivirals treatment in patients with chronic hepatitis C. J Med Virol. doi: 10.1002/jmv.26490
24. Chen J, Talwalkar JA, Yin M, Glaser KJ, Sanderson SO, Ehman RL (2011) Early detection of nonalcoholic steatohepatitis in patients with nonalcoholic fatty liver disease by using MR elastography. Radiology 259:749–756 [PubMed: 21460032]
25. Costa-Silva L, Ferolla SM, Lima AS, Vidigal PVT, Ferrari TCA (2018) MR elastography is effective for the non-invasive evaluation of fibrosis and necroinflammatory activity in patients with nonalcoholic fatty liver disease. European Journal of Radiology 98:82–89 [PubMed: 29279175]
26. Navin PJ, Hilscher MB, Welle CL, Mounajjed T, Torbenson MS, Kamath PS, Venkatesh SK (2019) The utility of MR elastography to differentiate nodular regenerative hyperplasia from cirrhosis. Hepatology 69 (1):452–454 [PubMed: 30014488]
27. Navin PJ, Gidener T, Allen AM, Yin M, Takahashi N, Torbenson MS, Kamath PS, Ehman RL, Venkatesh SK (2020) The Role of Magnetic Resonance Elastography in the Diagnosis of Noncirrhotic Portal Hypertension. Clin Gastroenterol Hepatol 18 (13):3051–3053.e3052. doi: 10.1016/j.cgh.2019.10.018 [PubMed: 31629882]
28. Cannella R, Giambelluca D, Pellegrinelli A, Cabassa P (2021) Color Doppler Ultrasound in Portal Hypertension: A Closer Look at Left Gastric Vein Hemodynamics. J Ultrasound Med 40 (1):7–14. doi: 10.1002/jum.15386 [PubMed: 32657462]
29. Asrani SK, Talwalkar JA, Kamath PS, Shah VH, Saracino G, Jennings L, Gross JB, Venkatesh SK, Ehman RL (2014) Role of magnetic resonance elastography in compensated and decompensated liver disease. Journal of Hepatology 60:934–939 [PubMed: 24362072]
30. Gidener T, Ahmed OT, Larson JJ, Mara KC, Therneau TM, Venkatesh SK, Ehman RL, Yin M, Allen AM (2020) Liver Stiffness by Magnetic Resonance Elastography Predicts Future Cirrhosis, Decompensation, and Death in NAFLD. Clin Gastroenterol Hepatol. doi: 10.1016/j.cgh.2020.09.044
31. Han MAT, Vipani A, Noureddin N, Ramirez K, Gornbein J, Saouaf R, Baniesh N, Cummings-John O, Okubote T, Setiawan VW, Rotman Y, Loomba R, Alkhouri N, Noureddin M (2020) MR elastography-based liver fibrosis correlates with liver events in nonalcoholic fatty liver patients: A multicenter study. Liver Int 40 (9):2242–2251. doi: 10.1111/liv.14593 [PubMed: 32652744]
32. Osman KT, Maselli DB, Idilman IS, Rowan DJ, Viehman JK, Harmsen WS, Harnois DM, Carey EJ, Gossard AA, LaRusso NF, Lindor KD, Venkatesh SK, Eaton JE (2020) Liver Stiffness Measured by Either Magnetic Resonance or Transient Elastography is Associated with Liver Fibrosis and is an Independent Predictor of Outcomes Among Patients With Primary Biliary Cholangitis. J Clin Gastroenterol. doi: 10.1097/MCG.0000000000001433
33. Eaton JE, Sen A, Hoodeshenas S, Schleck CD, Harmsen WS, Gores GJ, LaRusso NF, Gossard AA, Lazaridis KN, Venkatesh SK (2020) Changes in Liver Stiffness, Measured by Magnetic Resonance Elastography, Associated with Hepatic Decompensation in Patients with Primary Sclerosing Cholangitis. Clin Gastroenterol Hepatol 18 (7):1576–1583.e1571. doi: 10.1016/j.cgh.2019.10.041 [PubMed: 31683058]

34. Bae JS, Lee DH, Yi NJ, Lee KW, Suh KS, Kim H, Lee KB, Choi Y (2020) Magnetic Resonance Elastography Versus Transient Elastography in the Prediction of Complications After Resection for Hepatocellular Carcinoma. Ann Surg. doi: 10.1097/sla.0000000000004576
35. Lee DH, Lee JM, Yi NJ, Lee KW, Suh KS, Lee JH, Lee KB, Han JK (2017) Hepatic stiffness measurement by using MR elastography: prognostic values after hepatic resection for hepatocellular carcinoma. Eur Radiol 27:1713–1721 [PubMed: 27456966]
36. Ichikawa S, Motosugi U, Oguri M, Onishi H (2017) Magnetic resonance elastography for prediction of radiation-induced liver disease after stereotactic body radiation therapy. Hepatology 66 (2):664–665 [PubMed: 28218412]
37. Talwalkar JA, Yin M, Venkatesh SK, Rossman PJ, Grimm RC, Manduca A, Romano AJ, Kamath PS, Ehman RL (2009) Feasibility of in vivo MR elastographic splenic stiffness measurements in the assessment of portal hypertension. American Journal of Roentgenology 193:122–127 [PubMed: 19542403]
38. Dillman JR, Serai SD, Trout AT, Singh R, Tkach JA, Taylor AE, Blaxall BC, Fei L, Miethke AG (2019) Diagnostic performance of quantitative magnetic resonance imaging biomarkers for predicting portal hypertension in children and young adults with autoimmune liver disease. Pediatric Radiology 49:332–341 [PubMed: 30607435]
39. Alsaied T, Possner M, Lubert AM, Trout AT, Szugye C, Palermo JJ, Lorts A, Goldstein BH, Veldtman GR, Anwar N, Dillman JR (2019) Relation of Magnetic Resonance Elastography to Fontan Failure and Portal Hypertension. Am J Cardiol 124 (9):1454–1459. doi: 10.1016/j.amjcard.2019.07.052 [PubMed: 31474329]
40. Motosugi U, Ichikawa T, Koshiishi T, Sano K, Morisaka H, Ichikawa S, Enomoto N, Matsuda M, Fujii H, Araki T (2013) Liver stiffness measured by magnetic resonance elastography as a risk factor for hepatocellular carcinoma: a preliminary case–control study. Eur Radiol 23:156–162 [PubMed: 22814828]
41. Venkatesh SK, Yin M, Glockner JF, Takahashi N, Araoz PA, Talwalkar JA, Ehman RL (2008) MR elastography of liver tumors: preliminary results. American Journal of Roentgenology 190:1534–1540 [PubMed: 18492904]
42. Venkatesh SK, Hoodeshenas S, Venkatesh SH, Dispenzieri A, Gertz MA, Torbenson MS, Ehman RL (2019) Magnetic resonance elastography of liver in light chain amyloidosis. Journal of Clinical Medicine 8:739
43. Kim HJ, Kim B, Yu HJ, Huh J, Lee JH, Lee SS, Kim KW, Kim JK (2020) Reproducibility of hepatic MR elastography across field strengths, pulse sequences, scan intervals, and readers. Abdom Radiol (NY) 45 (1):107–115. doi: 10.1007/s00261-019-02312-9 [PubMed: 31720766]
44. Calle-Toro JS, Serai SD, Hartung EA, Goldberg DJ, Bolster BD, Darge K, Anupindi SA (2019) Magnetic resonance elastography SE-EPI vs GRE sequences at 3 T in a pediatric population with liver disease. Abdominal Radiology 44:894–902 [PubMed: 30600386]
45. Kim DW, Kim SY, Yoon HM, Kim KW, Byun JH (2019) Comparison of technical failure of MR elastography for measuring liver stiffness between gradient-recalled echo and spin-echo echo-planar imaging: a systematic review and meta-analysis. Journal of Magnetic Resonance Imaging
46. Yin M, Talwalkar JA, Glaser KJ, Venkatesh SK, Chen J, Manduca A, Ehman RL (2011) Dynamic postprandial hepatic stiffness augmentation assessed with MR elastography in patients with chronic liver disease. American Journal of Roentgenology 197:64–70 [PubMed: 21701012]
47. Hallinan JT, Alsaif HS, Wee A, Venkatesh SK (2015) Magnetic resonance elastography of liver: influence of intravenous gadolinium administration on measured liver stiffness. Abdominal Imaging 40:783–788 [PubMed: 25331568]
48. Plaikner M, Kremser C, Zoller H, Steurer M, Glodny B, Jaschke W, Henninger B (2019) Does gadoxetate disodium affect MRE measurements in the delayed hepatobiliary phase? European Radiology 29:829–837 [PubMed: 30027410]
49. Guglielmo FF, Venkatesh SK, Mitchell DG (2019) Liver MR elastography technique and image interpretation: pearls and pitfalls. RadioGraphics 39:1983–2002 [PubMed: 31626569]
50. Wang K, Manning P, Szeverenyi N, Wolfson T, Hamilton G, Middleton MS, Vaida F, Yin M, Glaser K, Ehman RL, Sirlin CB (2017) Repeatability and reproducibility of 2D and 3D hepatic

MR elastography with rigid and flexible drivers at end-expiration and end-inspiration in healthy volunteers. Abdominal Radiology 42:2843–2854 [PubMed: 28612163]

51. Choi SL, Lee ES, Ko A, Park HJ, Park SB, Choi BI, Cho YY, Kannengiesser S (2020) Technical success rates and reliability of spin-echo echo-planar imaging (SE-EPI) MR elastography in patients with chronic liver disease or liver cirrhosis. Eur Radiol 30 (3):1730–1737. doi: 10.1007/s00330-019-06496-y [PubMed: 31728687]
52. Kim DK, Yoon H, Han K, Kim J, Lee MJ, Kim S, Koh H, Han SJ, Shin HJ (2021) Effect of different driver power amplitudes on liver stiffness measurement in pediatric liver MR elastography. Abdom Radiol (NY). doi: 10.1007/s00261-021-03197-3
53. Manduca A, Bayly PJ, Ehman RL, Kolipaka A, Royston TJ, Sack I, Sinkus R, Van Beers BE (2021) MR elastography: Principles, guidelines, and terminology. Magn Reson Med 85 (5):2377–2390. doi: 10.1002/mrm.28627 [PubMed: 33296103]
54. Singh S, Venkatesh SK, Wang Z, Miller FH, Motosugi U, Low RN, Hassanein T, Asbach P, Godfrey EM, Yin M, Chen J, Keaveny AP, Bridges M, Bohte A, Murad MH, Lomas DJ, Talwalkar JA, Ehman RL (2015) Diagnostic performance of magnetic resonance elastography in staging liver fibrosis: a systematic review and meta-analysis of individual participant data. Clinical Gastroenterology and Hepatology 13:440–451 [PubMed: 25305349]
55. Kennedy P, Wagner M, Castera L, Hong CW, Johnson CL, Sirlin CB, Taouli B (2018) Quantitative elastography methods in liver disease: current evidence and future directions. Radiology 286 (3):738–763 [PubMed: 29461949]
56. Joshi M, Dillman JR, Towbin AJ, Serai SD, Trout AT (2017) MR elastography: high rate of technical success in pediatric and young adult patients. Pediatric Radiology 47:838–843 [PubMed: 28367603]
57. Serai SD, Trout AT (2019) Can MR elastography be used to measure liver stiffness in patients with iron overload? Abdominal Radiology 44:104–109 [PubMed: 30066167]
58. Ghoz HM, Kroner PT, Stancampiano FF, Bowman AW, Vishnu P, Heckman MG, Diehl NN, McLeod E, Nikpour N, Palmer WC (2019) Hepatic iron overload identified by magnetic resonance imaging-based T2* is a predictor of non-diagnostic elastography. Quant Imaging Med Surg 9 (6):921–927. doi: 10.21037/qims.2019.05.13 [PubMed: 31367546]
59. Gill HE, Lisanti CJ, Schwope RB, Kim J, Katz M, Harrison S (2021) Technical success rate of MR elastography in a population without known liver disease. Abdom Radiol (NY) 46 (2):590–596. doi: 10.1007/s00261-020-02652-x [PubMed: 32772122]
60. Silva AM, Grimm RC, Glaser KJ, Fu Y, Wu T, Ehman RL, Silva AC (2015) Magnetic resonance elastography: evaluation of new inversion algorithm and quantitative analysis method. Abdominal Imaging 40:810–817 [PubMed: 25742725]
61. Venkatesh SK, Ehman RL (2014) Magnetic resonance elastography of liver. Magn Reson Imaging Clin N Am 22:433–446 [PubMed: 25086938]
62. Motosugi U, Ichikawa T, Sano K, Sou H, Muhi A, Koshiishi T, Ehman RL, Araki T (2010) Magnetic resonance elastography of the liver: preliminary results and estimation of inter-rater reliability. Jpn J Radiol 28:623–627 [PubMed: 20972864]
63. Gandhi DB, Pednekar A, Braimah AB, Dudley J, Tkach JA, Trout AT, Miethke AG, Franck MD, Heilman JA, Dzyubak B, Lake DS, Dillman JR (2021) Assessment of agreement between manual and automated processing of liver MR elastography for shear stiffness estimation in children and young adults with autoimmune liver disease. Abdominal Radiology. doi: 10.1007/s00261-021-03073-0
64. Dzyubak B, Glaser K, Yin M, Manduca A, Ehman RL Automated Analysis of Hepatic MR Elastography Images with Motion Artifacts and Signal Inhomogenities. In: ISMRM, Salt Lake City, Utah, 2013.
65. Dzyubak B, Venkatesh SK, Manduca A, Glaser KJ, Ehman RL (2016) Automated liver elasticity calculation for MR elastography. Journal of Magnetic Resonance Imaging 43:1055–1063 [PubMed: 26494224]
66. Chen J, Allen AM, Therneau TM, Chen J, Li J, Hoodeshenas S, Chen J, Lu X, Zhu Z, Venkatesh SK, Song B, Ehman RL, Yin M (2021) Liver stiffness measurement by magnetic resonance elastography is not affected by hepatic steatosis. Eur Radiol. doi: 10.1007/s00330-021-08225-w

67. Yin M, Talwalkar JA, Glaser KJ, Manduca A, Grimm RC, Rossman PJ, Fidler JL, Ehman RL (2007) Assessment of hepatic fibrosis with magnetic resonance elastography. Clinical Gastroenterology and Hepatology 5:1207–1213 [PubMed: 17916548]
68. Leitao HS, Doblas S, Garteiser P, d'Assignies G, Paradis V, Mouri F, Geraldes CFGC, Ronot M, Van Beers BE (2017) Hepatic fibrosis, inflammation, and steatosis: influence on the MR viscoelastic and diffusion parameters in patients with chronic liver disease. Radiology 283 (1):98–107 [PubMed: 27788034]
69. Joshi M, Dillman JR, Singh K, Serai SD, Towbin AJ, Xanthakos S, Zhang B, Su W, Trout AT (2018) Quantitative MRI of fatty liver disease in a large pediatric cohort: correlation between liver fat fraction, stiffness, volume, and patient-specific factors. Abdominal Radiology 43:1168–1179 [PubMed: 28828531]
70. Mariappan YK, Dzyubak B, Glaser KJ, Venkatesh SK, Sirlin CB, Hooker J, McGee KP, Ehman RL (2017) Application of modified spin-echo-based sequences for hepatic MR elastography: evaluation, comparison with the conventional gradient-echo sequence, and preliminary clinical experience. Radiology 282 (2):390–398 [PubMed: 27509543]
71. Wang J, Glaser KJ, Zhang T, Shan Q, He B, Chen J, Yin M, Dzyubak B, Kugel JL, Kruse SA, Grimm RC, Venkatesh SK, Ehman RL (2018) Assessment of advanced hepatic MR elastography methods for susceptibility artifact suppression in clinical patients. Journal of Magnetic Resonance Imaging 47:976–987 [PubMed: 28801939]
72. Yin M, Glaser KJ, Talwalkar JA, Chen J, Manduca A, Ehman RL (2016) Hepatic MR elastography: clinical performance in a series of 1377 consecutive patients. Radiology 278 (1):114–124 [PubMed: 26162026]
73. Abe K, Takahashi A, Imaizumi H, Hayashi M, Okai K, Kanno Y, Sato N, Kenjo A, Marubashi S, Ohira H (2018) Utility of magnetic resonance elastography for predicting ascites in patients with chronic liver disease. Journal of Gastroenterology and Hepatology 33:733–740 [PubMed: 28834565]
74. Wagner M, Corcuera-Solano I, Lo G, Esses S, Liao J, Besa C, Chen N, Abraham G, Fung M, Babb JS, Ehman RL, Taouli B (2017) Technical failure of MR elastography examinations of the liver: experience from a large single-center study. Radiology 284 (2):401–412 [PubMed: 28045604]
75. Chen J, Yin M, Talwalkar JA, Oudry J, Glaser KJ, Smyrk TC, Miette V, Sandrin L, Ehman RL (2017) Diagnostic performance of MR elastography and vibration-controlled transient elastography in the detection of hepatic fibrosis in patients with severe to morbid obesity. Radiology 283 (2):418–428 [PubMed: 27861111]
76. Murphy IG, Graves MJ, Reid S, Patterson AJ, Patterson I, Priest AN, Lomas DJ (2017) Comparison of breath-hold, respiratory navigated and free-breathing MR elastography of the liver. Magnetic Resonance Imaging 37:46–50 [PubMed: 27746391]
77. Morin CE, Dillman JR, Serai SD, Trout AT, Tkach JA, Wang H (2018) Comparison of standard breath-held, free-breathing, and compressed sensing 2D gradient-recalled echo MR elastography techniques for evaluating liver stiffness. American Journal of Roentgenology 211:W279–W287 [PubMed: 30300003]
78. Wang H, Tkach JA, Trout AT, Dumoulin CL, Dillman JR (2019) Respiratory-triggered spin-echo echo-planar imaging-based MR elastography for evaluating liver stiffness. Journal of Magnetic Resonance Imaging 50:391–396 [PubMed: 30584687]
79. Boyarko AC, Dillman JR, Tkach JA, Pednekar AS, Trout AT (2021) Comparison of compressed SENSE and SENSE for quantitative liver MRI in children and young adults. Abdom Radiol (NY). doi: 10.1007/s00261-021-03092-x
80. Loomba R, Cui J, Wolfson T, Haufe W, Hooker J, Szeverenyi N, Ang B, Bhatt A, Wang K, Aryafar H, Behling C, Valasek MA, Lin GY, Gamst A, Brenner DA, Yin M, Glaser KJ, Ehman RL, Sirlin CB (2016) Novel 3D magnetic resonance elastography for the noninvasive diagnosis of advanced fibrosis in NAFLD: a prospective study. American Journal of Gastroenterology 111:986–994 [PubMed: 27002798]
81. Morisaka H, Motosugi U, Glaser KJ, Ichikawa S, Ehman RL, Sano K, Ichikawa T, Onishi H (2017) Comparison of diagnostic accuracies of two- and three-dimensional MR elastography of the liver. Journal of Magnetic Resonance Imaging 45:1163–1170 [PubMed: 27662640]

82. Wang J, Shan Q, Liu Y, Yang H, Kuang S, He B, Zhang Y, Chen J, Zhang T, Glaser KJ, Zhu C, Chen J, Yin M, Venkatesh SK, Ehman RL (2019) 3D MR elastography of hepatocellular carcinomas as a potential biomarker for predicting tumor recurrence. Journal of Magnetic Resonance Imaging 49:719–730 [PubMed: 30260529]

83. Shi Y, Qi YF, Lan GY, Wu Q, Ma B, Zhang XY, Ji RY, Ma YJ, Hong Y (2021) Three-dimensional MR Elastography Depicts Liver Inflammation, Fibrosis, and Portal Hypertension in Chronic Hepatitis B or C. Radiology 301 (1):154–162. doi: 10.1148/radiol.2021202804 [PubMed: 34374594]

84. Hirsch S, Guo J, Reiter R, Papazoglou S, Kroencke T, Braun J, Sack I (2014) MR elastography of the liver and the spleen using a piezoelectric driver, single-shot wave-field acquisition, and multifrequency dual parameter reconstruction. Magnetic Resonance in Medicine 71:267–277 [PubMed: 23413115]

85. Allen AM, Shah VH, Therneau TM, Venkatesh SK, Mounajjed T, Larson JJ, Mara KC, Schulte PJ, Kellogg TA, Kendrick ML, McKenzie TJ, Greiner SM, Li J, Glaser KJ, Wells ML, Chen J, Ehman RL, Yin M (2020) The Role of Three-Dimensional Magnetic Resonance Elastography in the Diagnosis of Nonalcoholic Steatohepatitis in Obese Patients Undergoing Bariatric Surgery. Hepatology 71 (2):510–521. doi: 10.1002/hep.30483 [PubMed: 30582669]

86. Dzyubak B, Glaser K, Yin M, Talwalkar J, Chen J, Manduca A, Ehman RL (2013) Automated liver stiffness measurements with magnetic resonance elastography. Journal of Magnetic Resonance Imaging 38:371–379 [PubMed: 23281171]

87. Dzyubak B, Venkatesh SK, Ehman RL Automated technique for hepatic MR Elastography analysis: comparison to skilled human interpretation. In: RSNA, Chicago, IL, 2013.

88. Dzyubak B, Venkatesh SK, Glaser K, Ehman RL Clinical Validation of a Semiautomated Workflow for MR Elastography. In: ISMRM, Paris, France, 2018.

89. Schwimmer JB, Behling C, Angeles JE, Paiz M, Durelle J, Africa J, Newton KP, Brunt EM, Lavine JE, Abrams SH, Masand P, Krishnamurphy R, Wong K, Ehman RL, Yin M, Glaser KJ, Dzyubak B, Wolfson T, Gamst AC, Hooker J, Haufe W, Schlein A, Hamilton G, Middleton MS, Sirlin CB (2017) Magnetic resonance elastography measured shear stiffness as a biomarker of fibrosis in pediatric nonalcoholic fatty liver disease. Hepatology 66 (5):1474–1485 [PubMed: 28493388]

90. Dzyubak B, Li J, Chen J, Mara KC, Therneau TM, Venkatesh SK, Ehman RL, Allen AM, Yin M (2021) Automated Analysis of Multiparametric Magnetic Resonance Imaging/Magnetic Resonance Elastography Exams for Prediction of Nonalcoholic Steatohepatitis. J Magn Reson Imaging 54 (1):122–131. doi: 10.1002/jmri.27549 [PubMed: 33586159]

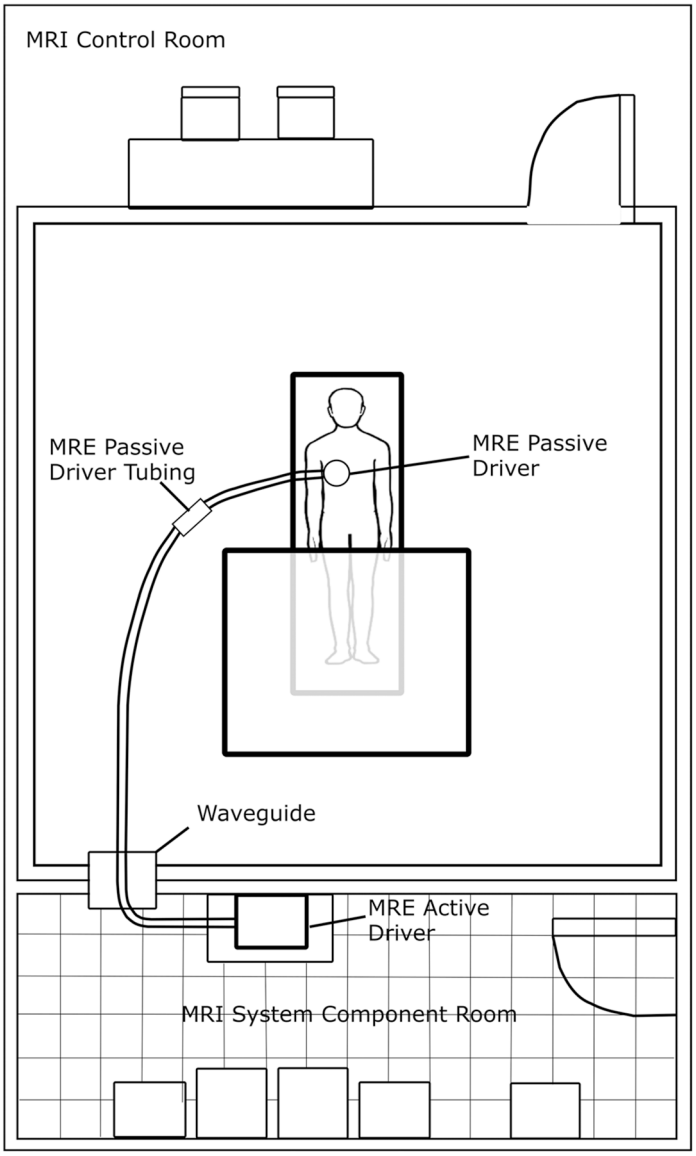

Fig. 1.

Diagram showing example MRI room set-up with active driver located in MRI system component room, passive driver tubing passing through the wave guide, and connection to passive driver. Subjects may be scanned feet-first supine (shown) or head-first supine (not-shown), depending on the requirements for the MRI system

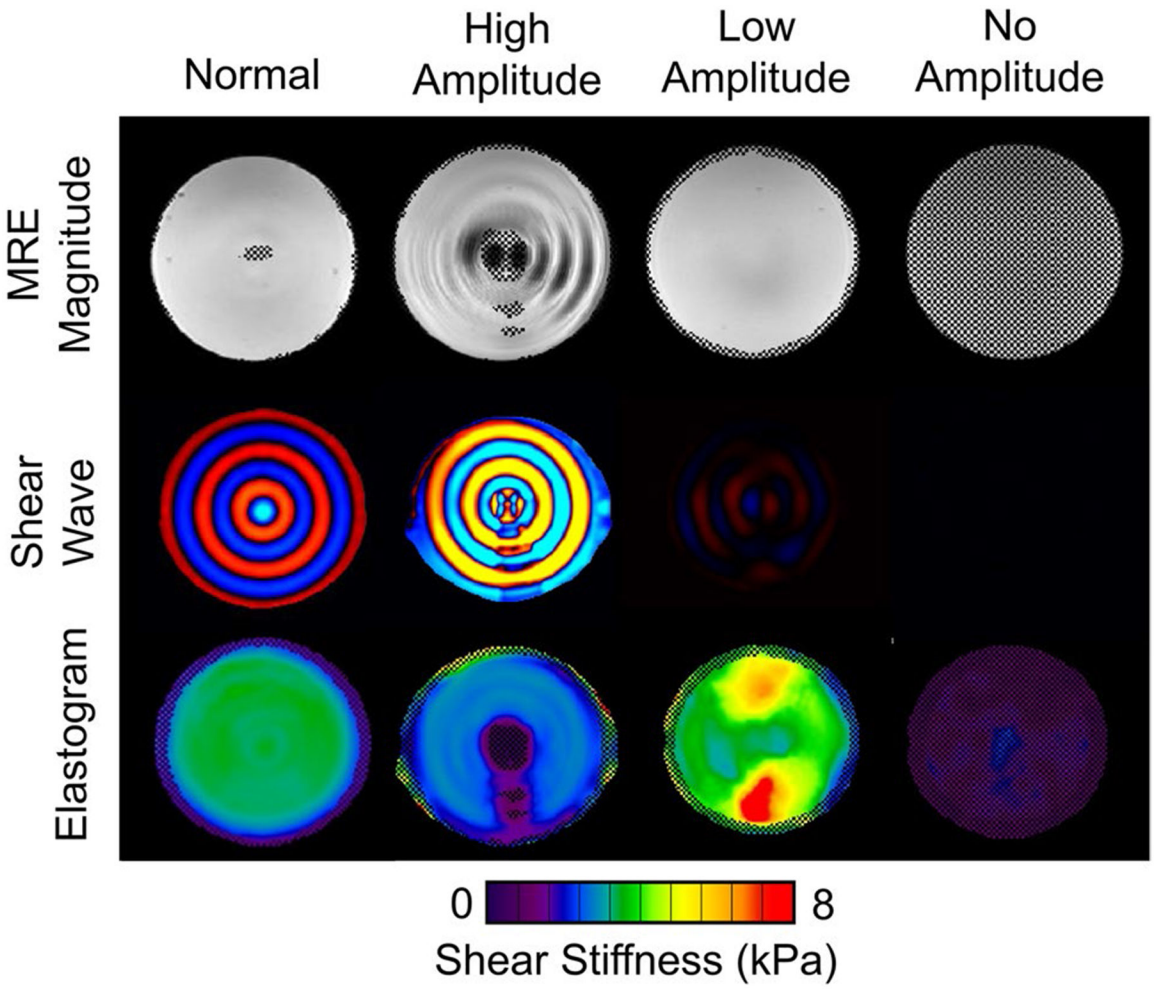

Fig. 2.

MRE phantom results. The MRE magnitude images (top), shear wave images (middle), and elastograms (bottom) are shown for four different acquisitions performed on the same phantom. Normal phantom results are shown in the left column. Typical examples of poor phantom results (from left to right) include an amplitude setting that is too high, too low, or no amplitude

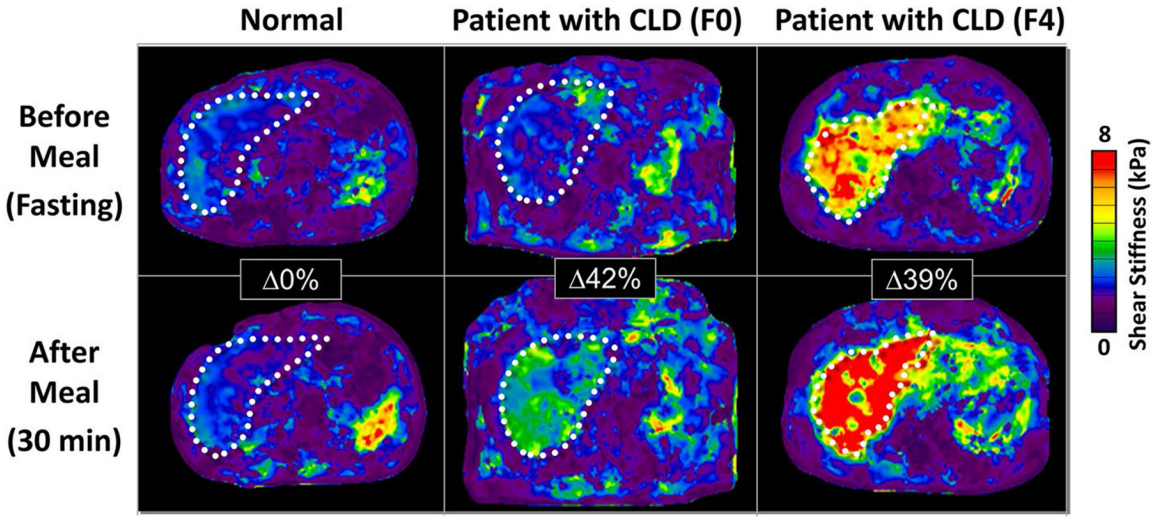

Fig. 3.

Examples of pre- and post-prandial hepatic MRE results demonstrating the importance of fasting. This figure shows the pre- and post-prandial MRE results in a normal healthy liver (left) and two patients with chronic liver disease and biopsy-proven fibrosis stages of F0 (middle) and F4 (right). There was no change in liver stiffness 30 min after a meal in the normal subject. For the patient with F0, there was a 42% increase in liver stiffness and for the patient with F4, a 39% increase

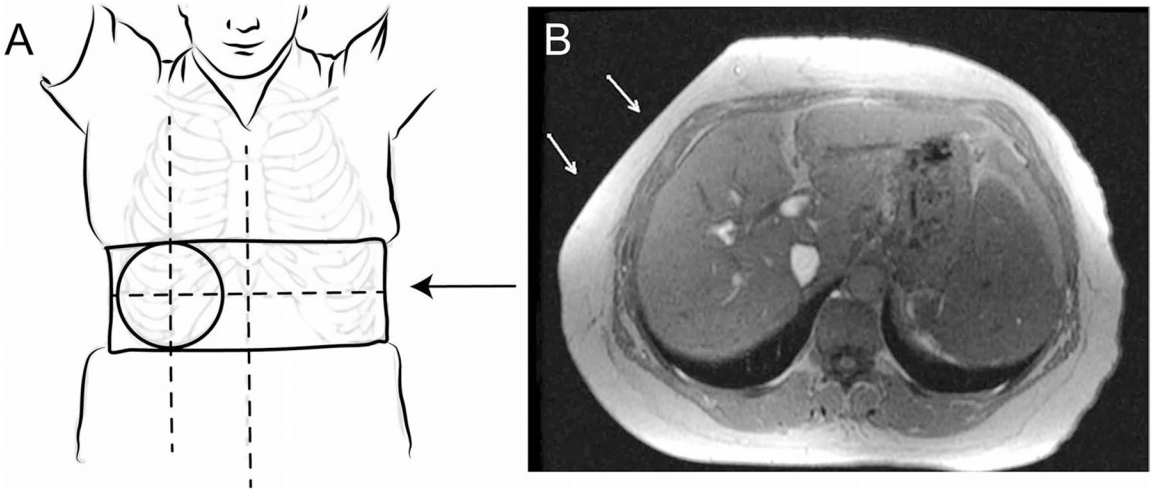

Fig. 4.

A Passive driver location: The passive driver should be centered at the level of the xiphoid process of the sternum, and the left–right position centered over the right midclavicular line. Note, the belt should be securely tightened (arrow). **B** Axial MR image showing indentation of the passive driver (arrows) on the subcutaneous fat in an obese subject. This is especially important in obese subjects, and some displacement of the abdominal fat is expected

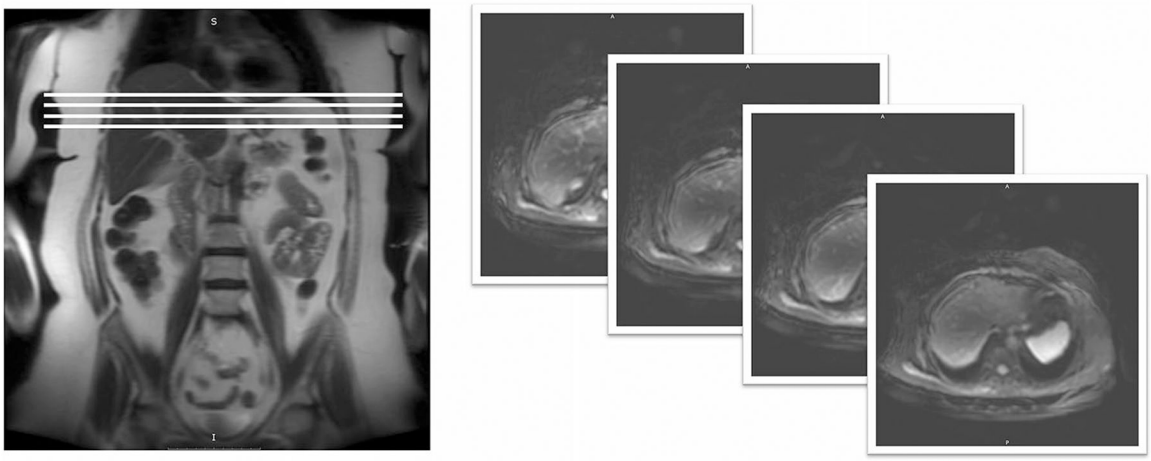

Fig. 5.

MRE section positioning, (left) coronal scout image demonstrating proper section positioning (white lines) in the widest cross-section of the liver. (Right) MRE magnitude images. Passive driver placement can often be seen as an indentation the subcutaneous fat

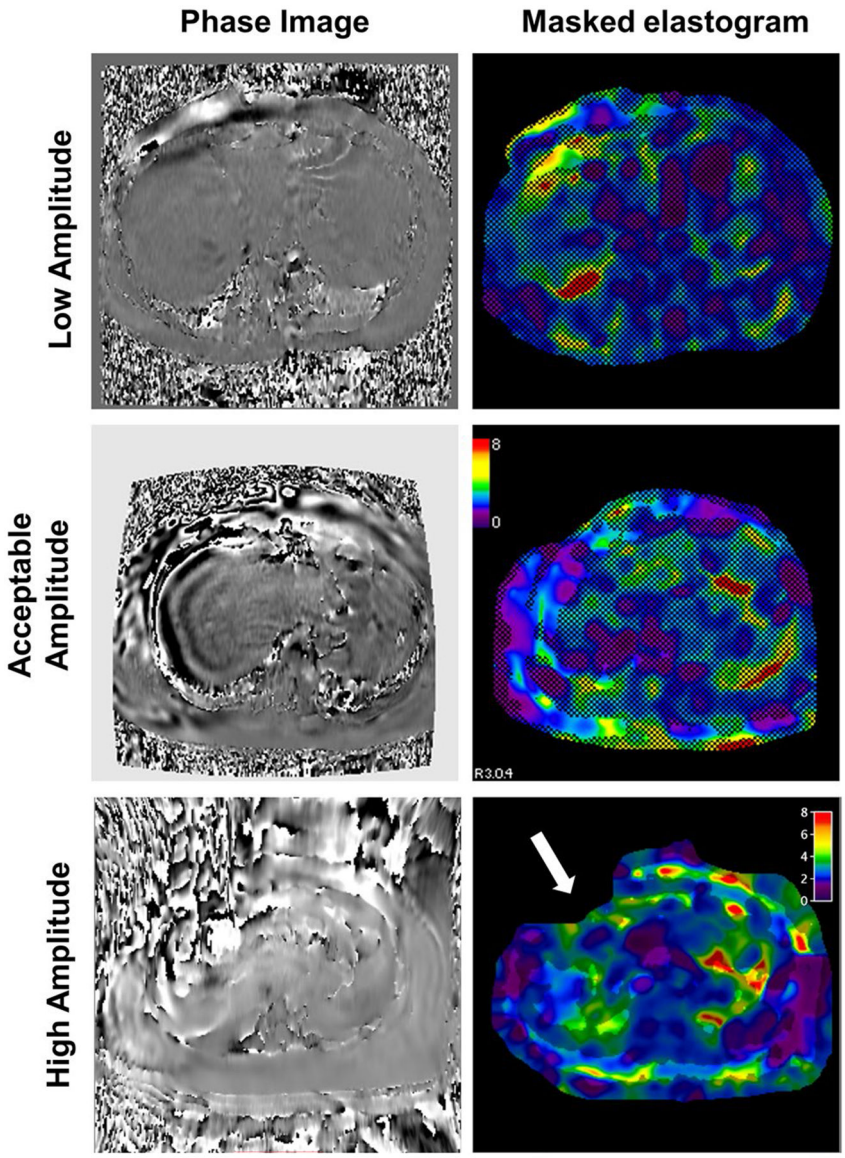

Fig. 6.

Examples of non-optimal amplitude settings: (Top) amplitude too low. Shear waves visible in the grayscale phase image (left) in the subcutaneous tissue and superficial anterior part of the liver but not in the rest of liver, and a very small region of high confidence in the masked elastogram (right). Amplitude should be increased, and the exam repeated. (Middle) acceptable shear wave amplitude. (Bottom) amplitude setting too high. Grayscale phase image appears noisy without a clear shear wave pattern (left), and a small region of high confidence and part of the body masked out (black shading in this example) due to too much motion (white arrow) (right). Amplitude should be reduced, and the exam repeated

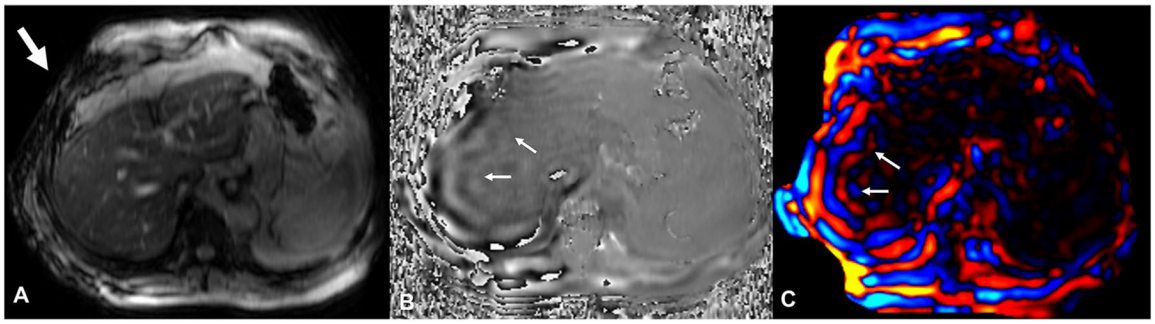

Fig. 7.

Verification of shear wave delivery to the liver: On the magnitude images (**A**), acoustic wave delivery from the passive driver to the abdomen can be seen as signal loss in the subcutaneous fat just below the passive driver (arrow, **A**) due to intravoxel phase dispersion. The propagating shear waves through the liver can be verified on the phase images (**B**) as alternate bands (arrows). On the wave images (**C**), the planar (in the plane of the slice) propagation of the shear waves appears as parallel bands of blue and red waves (arrows)

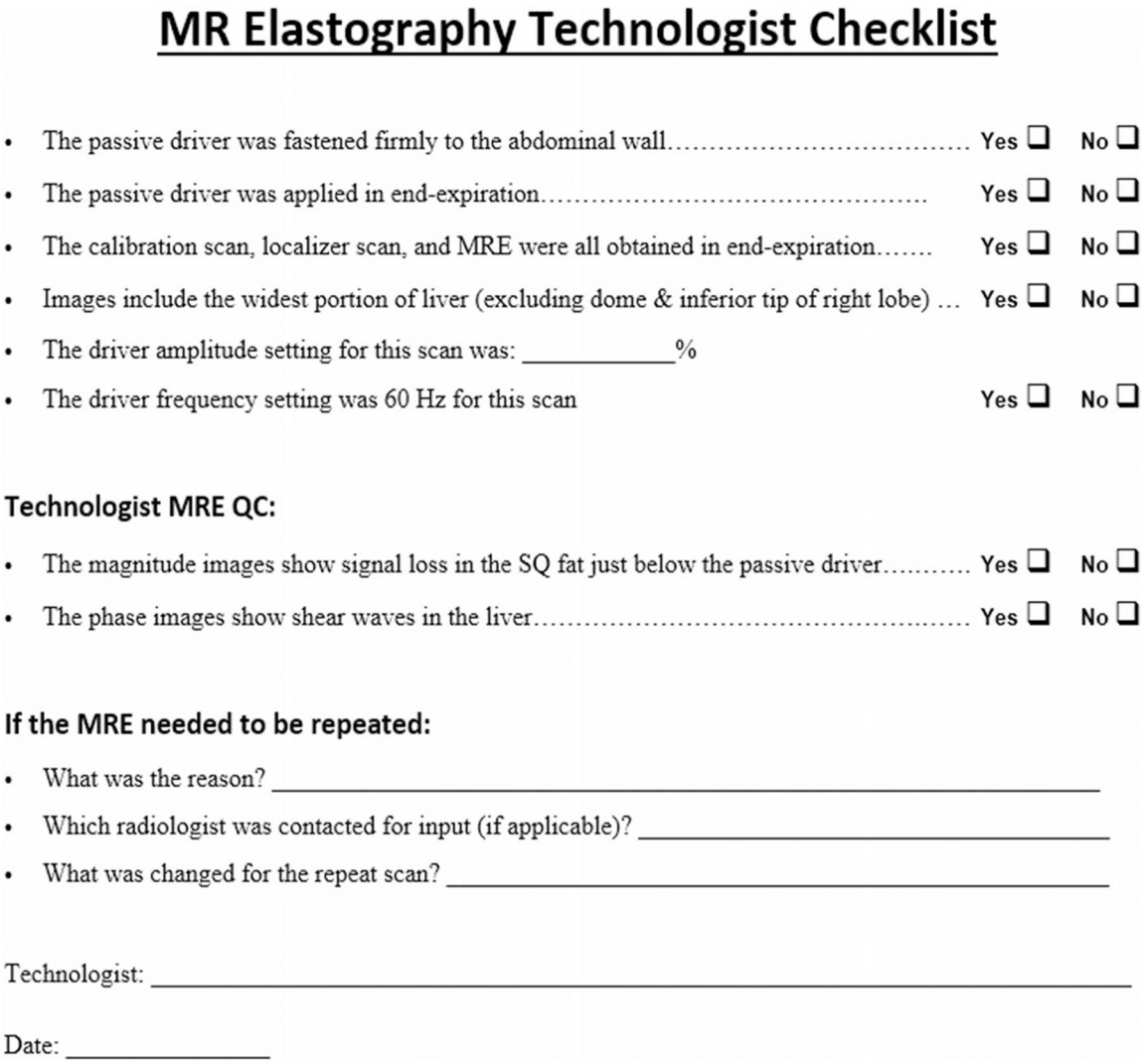

MR Elastography Technologist Checklist

- The passive driver was fastened firmly to the abdominal wall..... Yes ❑ No ❑
- The passive driver was applied in end-expiration..... Yes ❑ No ❑
- The calibration scan, localizer scan, and MRE were all obtained in end-expiration..... Yes ❑ No ❑
- Images include the widest portion of liver (excluding dome & inferior tip of right lobe) ... Yes ❑ No ❑
- The driver amplitude setting for this scan was: _____%
- The driver frequency setting was 60 Hz for this scan Yes ❑ No ❑

Technologist MRE QC:

- The magnitude images show signal loss in the SQ fat just below the passive driver..... Yes ❑ No ❑
- The phase images show shear waves in the liver..... Yes ❑ No ❑

If the MRE needed to be repeated:

- What was the reason? _____
- Which radiologist was contacted for input (if applicable)? _____
- What was changed for the repeat scan? _____

Technologist: _____

Date: _____

Fig. 8.

MRE Technologist Checklist to ensure a successful exam. This QC checklist can be completed after every MRE exam by the MR technologist. *SQ* subcutaneous. Modified with permission from Guglielmo et al. [49]

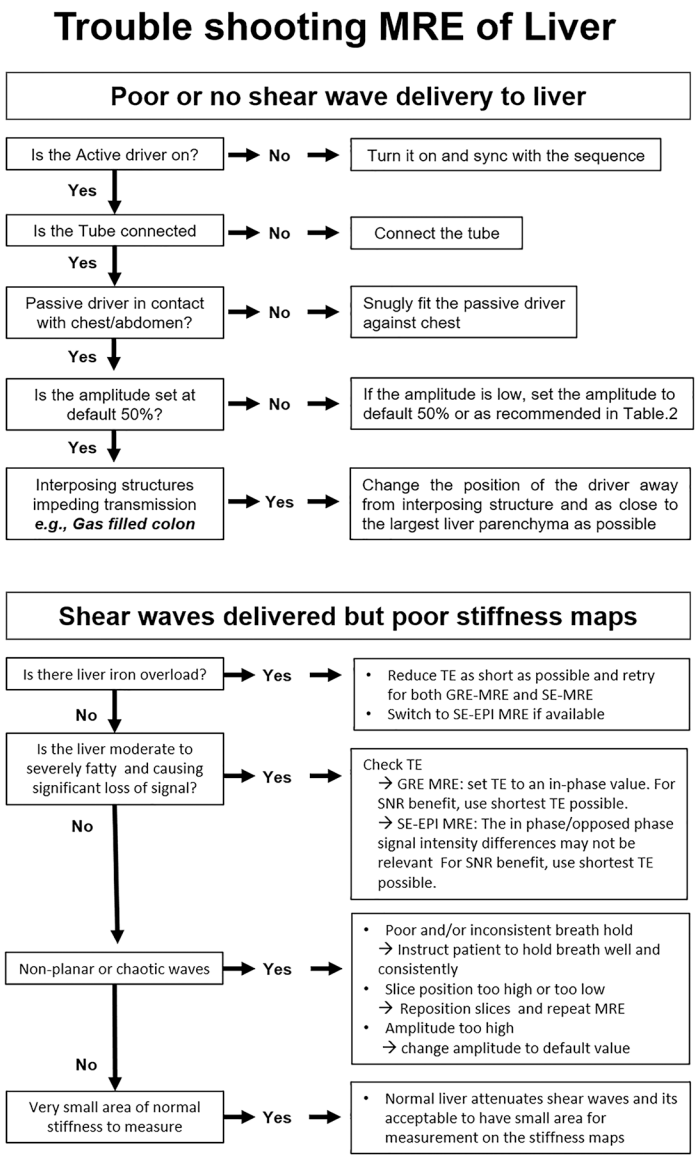

Fig. 9.

Flow chart illustrating troubleshooting tips for MR technologists performing a clinical liver MRE study

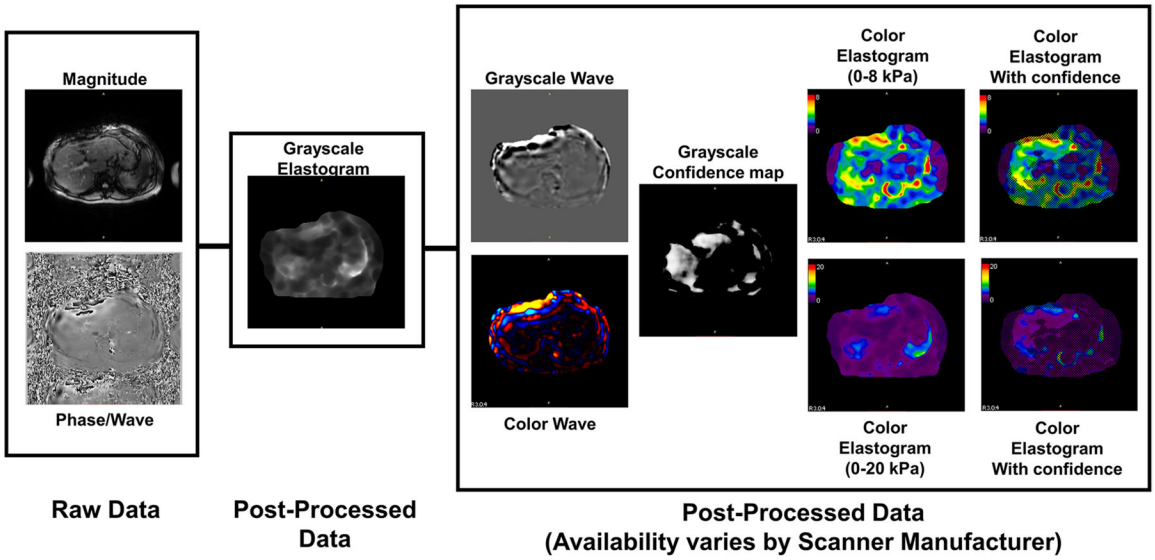

Fig. 10.

Raw and post-processed images available for analysis: The raw images from a liver MRE are the magnitude and phase/wave images used for anatomic information and shear wave propagation, respectively. The grayscale elastogram should be used for quantitative interpretation and is available from all scanner manufacturers. The box to the right indicates alternative presentations of the data, including grayscale and color variations of the wave data and elastogram images, but are non-quantitative

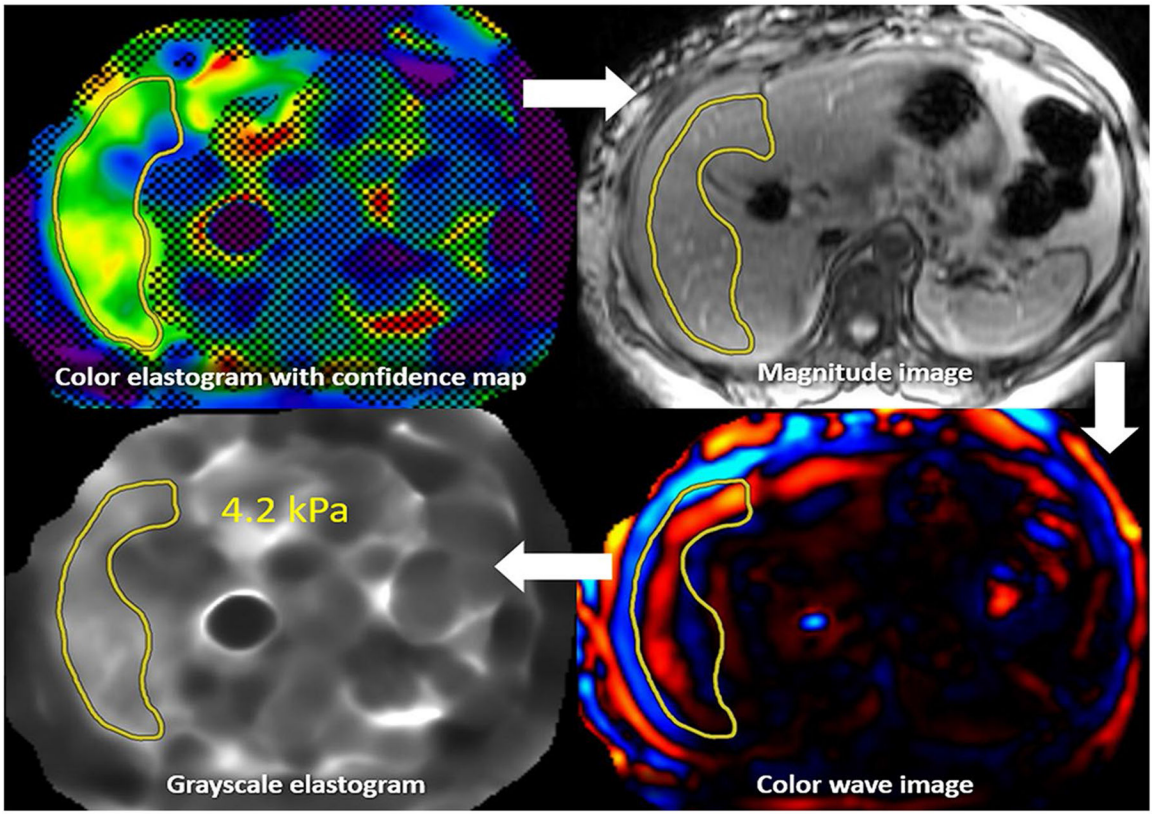

Fig. 11.

MRE interpretation with confidence map: An ROI is first drawn on the color elastogram with confidence map. This ROI is then copied to the magnitude image, with alterations made to ensure only the liver is being sampled. This ROI is then copied to the color wave image, where alterations can be made to ensure only good-quality waves are being sampled. Finally, the ROI can be copied to the grayscale elastogram, with the ROI value representing liver stiffness. The process is repeated for all four slices, and a weighted arithmetic mean calculated. This patient's liver stiffness of 4.2 kPa corresponds to the stage 3–4 fibrosis range, in the appropriate clinical setting

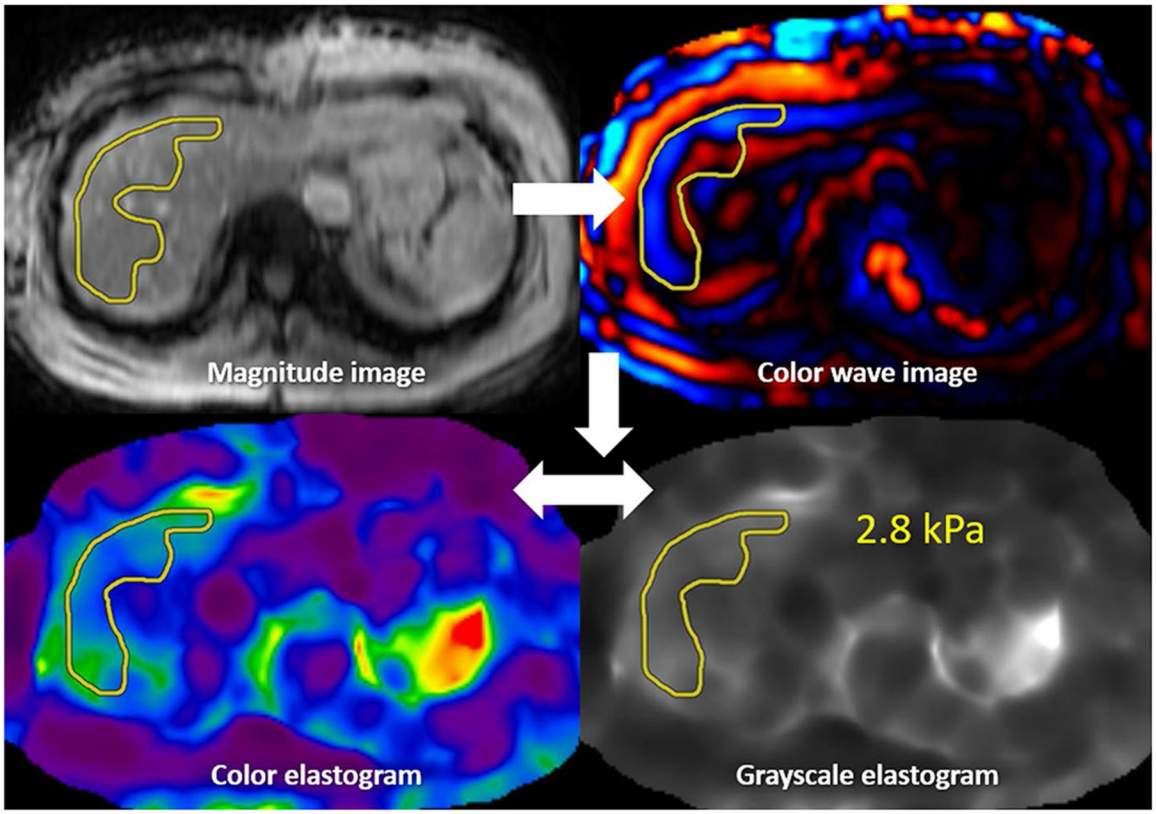

Fig. 12.

MRE interpretation without confidence map: An ROI is first drawn on the magnitude image. This ROI is then copied to the color wave image, where alterations can be made to ensure only good-quality waves are being sampled. This ROI can then be copied to the color or grayscale elastogram, with the ROI value representing liver stiffness. The process is repeated for all four slices, and then a weighted arithmetic mean calculated. This patient's liver stiffness of 2.8 kPa is in the normal/inflammation range

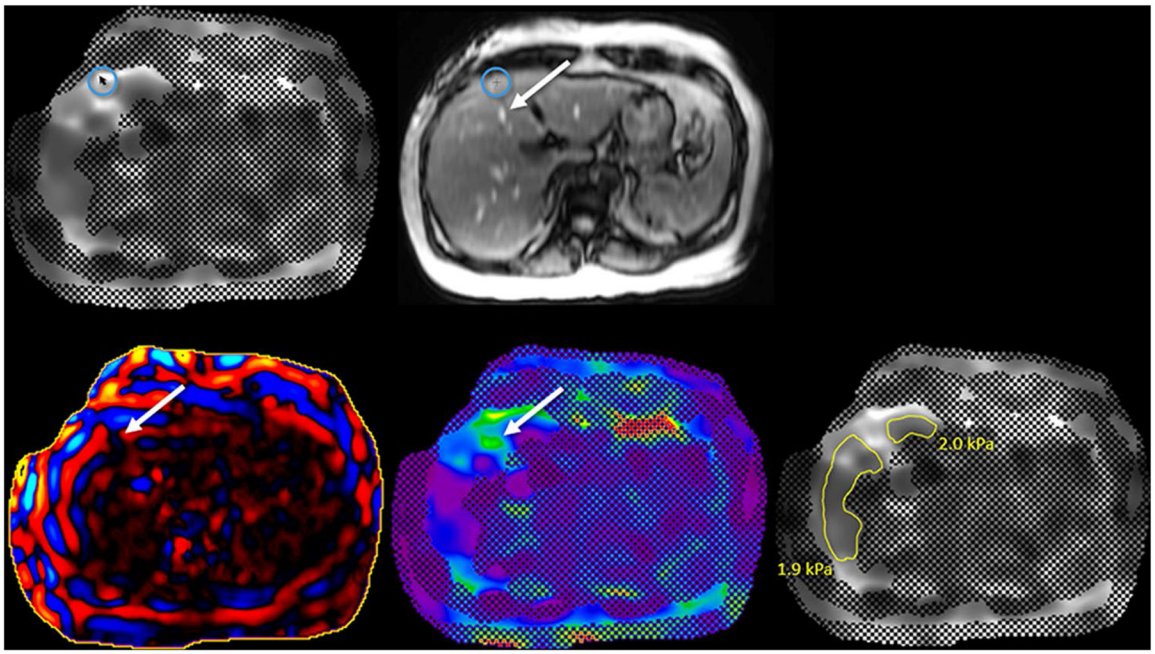

Fig. 13.

Liver stiffness measurements with a confidence map but no copy/paste function. The grayscale elastogram with confidence map image is first reviewed (**A**). If a "localizer mode" is available, when the mouse is hovered over the elastogram image (circle in **A**), a crosshair appears on the magnitude image (circle in **B**) indicating where the measurements are being obtained so the peripheral liver, large blood vessels (arrow in **B**), etc. can be avoided. Next, the wave image (**C**) is reviewed to exclude areas of wave distortion (arrow in **C**) or poor wave propagation. The color elastogram is then reviewed for artifactual "hot spots" (arrow in **D**) which may overestimate liver stiffness. The hot spot in image **D** (arrow) is caused by large blood vessels (arrow in **B**). After reviewing all four series, freehand ROI measurements are made on the grayscale elastogram (**E**). The process is repeated for all four slices, and then a weighted arithmetic mean calculated. On this slice, the liver stiffness measurements of 1.9 kPa and 2.0 kPa are in the normal range

Table 1

Indications for liver MRE

Evaluation of liver fibrosis in chronic liver disease (CLD) • Diagnosis • Staging • Longitudinal monitoring
Assessment of treatment response Longitudinal monitoring • For development of fibrosis in patients receiving drugs that can cause liver fibrosis (e.g., methotrexate) • Congestive hepatopathies—progressive increasing stiffness over time suggests worsening fibrosis or increasing congestion • Decrease in liver stiffness following therapeutic intervention (e.g., HCV, NAFLD)
Emerging applications • Differentiate non-alcoholic fatty liver (simple steatosis) from non-alcoholic steatohepatitis • Differentiate non-cirrhotic portal hypertension (NCPH) from cirrhotic portal hypertension (CPH)
Possible applications • Prediction of decompensation and outcome in CLD patients on clinical follow-up, CLD patients undergoing hepatectomy or localized radiation treatment • Differentiation of benign and malignant liver tumors • Other diffuse disorders that increase liver stiffness, such as amyloidosis

Table 2

MRI scan parameters for 2D MRE

Series	GE 1.5 T	GE 3.0 T	Philips 1.5 T		Philips 3.0 T		Siemens 1.5 T		Siemens 3.0 T	
	2D GRE MRE	2D SE-EPI MRE	2D GRE MRE	2D SE-EPI MRE	2D GRE MRE	2D SE-EPI MRE	2D GRE MRE	2D EPI MRE	2D GRE MRE	2D EPI MRE
Software version			≥ 5.1.7	≥ 5.6.1	≥ 5.1.7	≥ 5.6.1	< VE11E	≥ VE11E	< VE11E	≥ VE11E
Plane	Axial	Axial	Axial	Axial	Axial	Axial	Axial	Axial	Axial	Axial
Pulse sequence	MR-Touch	MR-Touch (EPI)	FFE MRE	SEEPI	FFE MRE	SEEPI	greMRE	epseMRE	greMRE	epseMRE
TR (ms)	50	1000	50	1000	50	1000	50	1000	50	1000
TE (ms)	MinTE (~ 18.2)	MinFULL (~ 55.4)	20	Min (~ 58)	20	Min (~ 58)	Min (~ 20)	Min	Min (~ 20)	Min
Bandwidth	31.25 kHz	250 kHz	288 Hz/pixel	2000 Hz/pixel	288 Hz/pixel	2000 Hz/pixel	260 Hz/pixel	~ 2000 Hz/pixel	260 Hz/pixel	~ 2380 Hz/pixel
Field of view (mm)	420×420	420×420	450×403	420×420	450×403	420×420	420×420	420×420	420×420	420×420
Number of slices	4	4	4	4	4	4	4	4	4	4
Thickness (mm)	10	8	10	8	10	8	10	8 mm/25%	10	8 mm/25%
Slice gap (mm)	0	2	1	2	1	2	0	2 mm	0	2 mm
Fat suppression	On	On	On	On	On	On	On	On	On	On
NEX, NSA	1	1	1	1	1	1	1	1	1	1
Acquisition matrix	256×64	80×80	300×85	100×100	300×85	100×100	256×64	98×100% (98)	256×64	98×100% (98)
Frequency-encoding direction	R/L	R/L	R/L	R/L	R/L	R/L	R–L	R–L	R–L	R×L
Flip angle (°)	25	90	30	90	30	90	20	90	20	90
Typ. scan time (s)	55 (For 4 slices)	16 (Per slice)	71 (For 4 slices)	9	71 (For 4 slices)	9	17 (Per slice)	11	17 (Per slice)	11
MRE driver frequency (Hz)	60	60	60	60	60	60	60	60	60	60
MEG frequency (Hz) (or period mismatch)	60 Hz	60 Hz	60 Hz	60 Hz	60 Hz	60 Hz	80%	80%	80%	80%
Axis of MEG	4 (Z)	4 (Z)	FH	FH	FH	FH	Slice	Slice	Slice	Slice
Comments	Sat bands: S/I Options: ASSET, fast,	Sat bands: S/I Options: ASSET, fast,	REST slabs: 2 parallel Center	Shimming volume: auto	REST slabs: 2 parallel Center	Shimming volume: auto	Sat bands: S/I Center	Sat bands: S/I GRAPPA×2 Resolution: filter	Sat bands: S/I Center	Sat bands: S/I GRAPPA×2 Resolution: filter

Series	GE 1.5 T	GE 3.0 T	Philips 1.5 T		Philips 3.0 T		Siemens 1.5 T		Siemens 3.0 T	
	2D GRE MRE	2D SE-EPI MRE	2D GRE MRE	2D SE-EPI MRE	2D GRE MRE	2D SE-EPI MRE	2D GRE MRE	2D EPI MRE	2D GRE MRE	2D EPI MRE
	multiphase Center frequency on water peak	multiphase Center frequency on water peak	frequency on water peak		frequency on water peak		frequency on water peak	Image: prescan Normalize Center frequency on water peak	frequency on water peak	Image: prescan Normalize Center frequency on water peak

GRE gradient echo, *EPI* echo planar imaging, *SE-EPI* spin echo-echo planar imaging, *TR* repetition time, *TE* echo time, *NEX* number of excitations, *NSA* number of signals averaged, *MEG* motion-encoding gradients, *ASSET* array coil spatial sensitivity encoding, *REST* regional saturation technique, *GRAPPA* generalized autocalibrating partial parallel acquisition, *FH* foot head, *R/L* right/left, *MRE* magnetic resonance elastography

Table 3

MRE sequence parameters for clinical liver MRE

Fixed parameters (should not be changed)	Consistent parameters (for same patient)	Flexible parameters (adjustable as needed)
Pulse frequency (default 60 Hz)	Field of view (FOV) at baseline and follow-up (420×420 mm recommended)	Driver amplitude (default at 50%)
Motion-encoding gradient (MEG) direction (default *z*-direction)	Section positioning (try to achieve same anatomical coverage for follow-up scans)	Time to echo (TE)—ideally in-phase
Number of phase offsets (default four phase offsets)	Breathing technique (end-expiration strongly recommended, but if not possible can be done at inspiration)	
Imaging plane (axial)		
Imaging acceleration		

Table 4

Proposed MRE amplitude recommendations

Patient profile		Setup instructions	Amplitude recommendations		
			Rigid driver	**Flex driver, small**	**Flex driver, large**
Small[a,b]	< 57 kg (125 lbs) *or* BMI < 20 *or* Petite body stature	Ensure center of passive driver positioned correctly. Edges of the passive driver may not contact the body surface in very small patients	**30%** (20–40%)	**30%** (25–45%)	**40%** (30–50%) *Not common*
Normal	57–75 kg (125–170 lbs) *or* BMI: (20–25)	Follow standard set-up instructions	**40%** (30–50%)	**40%** (30–50%) *Not common*	**50%** (40–60%)
Large[c]	> 75 kg (170 lbs) *or* BMI > 25 *or* high abdominal habitus	Apply additional tension to the belt to compact adipose fat layer as much as patient comfort will allow	**60%** (50–80%)	**60%** (50–80%) *Not common*	**70%** (50–80%)

Starting amplitude given for each patient profile in bold font, along with range to adjust if initial results are poor

[a]Recommended amplitudes are lowered primarily for comfort and to prevent over-driving near the passive driver

[b]For patients < 23 kg (50 lbs), amplitudes may need to be lowered further for patient comfort and to prevent over-driving, resulting in signal loss below the driver and poor image quality

[c]Amplitudes are increased to ensure vibrations penetrate adipose fat

Table 5

MR elastography active driver amplitude setting guidelines for the pediatric population

Patient weight (kg)	Driver amplitude (starting value) (%)
< 20	5–10
20–29	10–20
30–39	20–30
40–59	30–40
60–69	50
70–85	60
86–99	70
≥ 100	80

The above recommendations are provided as guidelines. The optimal active driver amplitude also will be influenced by patient body habitus and body mass index. If there is excessive phase wrap and associated signal loss on the phase and magnitude MR elastography images, the driver amplitude should be reduced and imaging repeated. Alternatively, if wave penetration is poor and/or chaotic, the driver amplitude should be increased and imaging repeated

Table 6

Data output available by scanner type

	GE	Philips	Siemens
Acquired data			
Magnitude[1]	Y	Y	Y
Phase difference[1]	Y	Y	Y
Post-process data			
Stiffness, grayscale, 0–8 kPa	Y	Y[5]	Y
Stiffness, grayscale, 0–8 kPa, w/ confidence overlay[2]	Y	Y[5]	Y
Stiffness, RGB, 0–8 kPa	Y[6]	Y[5]	N[3]
Stiffness, RGB, 0–8 kPa, w/ confidence overlay	Y[6]	Y[5]	N[3]
Wave, grayscale	N	N	Y
Wave, RGB	Y[6]	Y[5]	N[3]
Confidence map (0–1)[4]	N	Y	Y

Unless otherwise noted below, the following table describes the data that each scanner is able to export for MRE results. In some cases, the users may have to select this to be included in the output, as it is not included by default

[1] GE and Philips combine phase and magnitude images into a single series. Siemens saves them as separate, consecutive series

[2] Images with confidence overlay will create a hatch-out by setting the pixel values to “0,” and in the case of grayscale images, including a portion of this area in an ROI will yield incorrect quantitative results

[3] All Siemens outputs are grayscale. RGB images can be created by manually configuring a series to colorize them and export

[4] Confidence map is a number in the range 0–1. Confidence overlays are created by thresholding the map at 0.95 for GRE sequences and ~ 0.98 for SE-EPI sequences

[5] Philips post-processed images are only created when/if the MREview tool is invoked on-scanner

[6] GE RGB images are effectively screenshots and will contain patient name and related information in the pixel data

Table 7

Interpretation of MRE results

Mean liver stiffness	Fibrosis stage
< 2.5 kPa	Normal
2.5 to 3.0 kPa	Normal or inflammation
3.0 to 3.5 kPa	Stage 1–2 fibrosis
3.5 to 4.0 kPa	Stage 2–3 fibrosis
4.0 to 5.0 kPa	Stage 3–4 fibrosis
> 5.0 kPa	Stage 4 fibrosis or cirrhosis

Values above 3.0 kPa are consistent with liver fibrosis in the appropriate clinical setting for exams obtained at both 1.5 and 3.0 T using both GRE and SE-EPI acquisitions

The liver stiffness values must be interpreted in the clinical context to rule out congestion, severe active inflammation, severe biliary obstruction. See Interpretation Tips